

# TROPOSPHERIC PROPAGATION ERRORS IN RADAR MEASUREMENTS FOR INDIA

A Thesis Submitted  
In Partial Fulfilment of the Requirements  
for the Degree of  
MASTER OF TECHNOLOGY

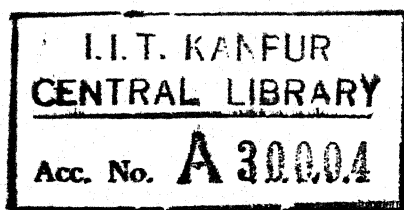
By  
SQN. LDR. K. D. S. BALI

to the

DEPARTMENT OF ELECTRICAL ENGINEERING  
INDIAN INSTITUTE OF TECHNOLOGY KANPUR  
JULY 1974

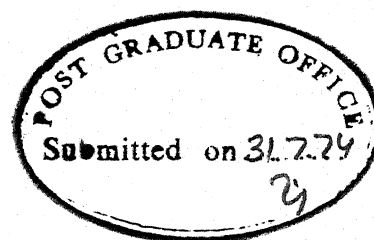
To my parents - Sardar and Sardarni  
Balwant Singh Bali for their affectionate  
guidance and constant encouragement.

Thesis  
621.3848  
B 198



27 AUG 1974

EE-1974-M-BAL-TRO



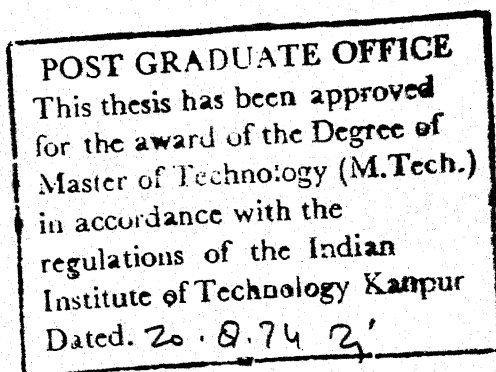
CERTIFICATE

This is to certify that the thesis entitled, 'Tropospheric propagation errors in radar measurements for India' is a record of the work carried out under my supervision and that it has not been submitted elsewhere for a degree.

*N. Singh*  
31.7.74

Dr. N. Singh  
Assistant Professor  
Department of Electrical Engineering  
Indian Institute of Technology  
Kanpur

July 1974.

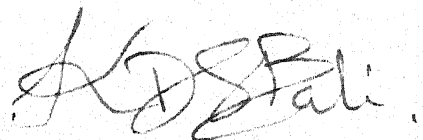




ACKNOWLEDGEMENT

I am extremely indebted to my thesis advisor, Dr. N. Singh, for constant inspiration, guidance and freely giving his time for discussion throughout this work. I also thank him for his valuable suggestions and help provided to me from time to time.

Thanks are also due to the staff of Computer Center and my colleagues for valuable help for computer work. Finally Mr. K.N. Tewari deserves special mention for his excellent and neat typing work.

A handwritten signature in dark ink, appearing to read 'K.D.S. Bali', with a stylized, cursive script.

K.D.S. Bali

## TABLE OF CONTENTS

	Page
Abstract	vii
CHAPTER I      INTRODUCTION	1
1.1    Background and motivation	1
1.2    Radio refractive index of air	2
1.3    Surface and sea level refractivity	4
1.4    Reference atmosphere	5
1.5    Elevation angle and radar range errors	6
CHAPTER II     DETERMINATION OF RADAR MEASUREMENT ERRORS	8
2.1    Introduction	8
2.2    Tropospheric refraction effects on em waves	10
2.3    Evaluation of ray    bending	12
2.4    Methods for determining elevation and range errors	21
CHAPTER III    A COMPUTER PROGRAM FOR ERROR CALCULATION	22
3.1    Introduction	22
3.2    A numerical integration method	23
3.3    The computational method	30
CHAPTER IV     CALCULATIONS AND RESULTS	32
4.1    Introduction	32
4.2    Tables for radar measurement    errors	32
4.3    Error    Curves	34

4.4 Radar coverage diagrams	50
4.5 Height versus error curves	50
CHAPTER V NUMERICAL SIMULATION OF TROPOSPHERE OVER DELHI BY MONTE-CARLO TECHNIQUES	61
5.1 Introduction	61
5.2 Setup for simulation of troposphere	62
5.3 Results	62
CHAPTER VI DISCUSSION OF RESULTS AND CONCLUSION	65
APPENDIX A	67
APPENDIX B	73
REFERENCES	75

ABSTRACT

✓ Radar range and elevation angle errors which arise due to the refractivity variations of the troposphere have been discussed in this thesis. Eight radio sonde stations, namely, Delhi Allahabad, Jodhpur, Nagpur, Bombay, Calcutta, Madras and Trivandrum are considered. Error calculations are based on the known average monthly surface refractivity values of these places. ✓ Such errors are of considerable importance for long range surveillance radar systems which are used for the detection of long range airborne targets, missiles and satellites.]

✓ A numerical integration technique along with the negative exponential profile for refractivity variation with height has been used for finding the errors. ✓ The height and the ground range of the target are also found out by this method. ✓ The surface refractivity,  $N_s$ , is converted to  $N_0$ , the refractivity at sea level, for avoiding the altitude dependence of  $N_s$  and for better presentation. A target varying in range from 10 Kms to 600 Kms and in elevation angle from  $0.5^\circ$  to  $75^\circ$  is assumed for finding the theoretical values of elevation angle and range errors.)

[ It is found that the elevation angle and the range errors of the target increase with increase in range and decrease with increasing elevation angle. One way maximum radar range error is found out to be varying from 114 meters to 119 meters for Delhi, Nagpur, Allahabad and Jodhpur for July/August, 116 meters for Madras for October and Trivandrum for May, and from 119 meters ]

to 120 meters for Bombay and Calcutta for June. The elevation angle error is found out to be nearly  $0.4^{\circ}$  for Delhi and Nagpur for September, Allahabad for August, Jodhpur for July, Madras and Bombay for April, Calcutta for May and Trivandrum for June.

Monte-Carlo technique is used for numerical simulation of troposphere over Delhi by generating 1000 normally distributed pseudorandom ( $N_s$ ) numbers and these are then used for finding the elevation angle and the range errors for the target. Mean and standard deviation for elevation angle and range errors have been calculated and their density distributions are given.

## CHAPTER I

### INTRODUCTION

#### 1.1 Background and Motivation

An important consideration which must be taken into account for any radar system is the degradation in the signal-target information due to the refractivity variations in the earth's atmosphere. Signal deterioration is caused by spatial inhomogeneities in the atmosphere which are continuously varying with time. These spatial variations produce statistical bias errors while the time varying components results in fluctuating or rms inaccuracies. These effects result in refractivity bending, time delays, doppler errors, rotation of the plane of polarization, dispersion effects and the attenuation of the signal. The first two of these result in elevation angle and range measurement errors of the target, respectively, and these two are analysed in this thesis.

In general, the regions of the atmosphere which affect the propagation of em waves are the troposphere and the ionosphere. Troposphere is a nondispersive medium as the refractivity variations and hence the tropospheric refraction effects are frequency independent upto 100 GHz [1], thus affecting the performance of most of the operational radar systems. Such effects are relatively unimportant for short range airborne radar systems such as weapon control radar, side looking terrain mapping radar and weather

avoidance radar. On the other hand, tropospheric refraction effects are of great importance in long range surveillance radar systems. However, on the other hand, ionosphere is a dispersive medium as its refractive index is frequency dependent and at sufficiently low frequencies, the ionosphere is birefringent and anisotropic and a simple Snell's law approach is invalid.

While a lot of work has been done in the other countries in this field, particularly by National Bureau of Standards, U.S.A.; hardly any work has so far been reported in India. In the ensuing discussion, the ionospheric effects have been ignored by assuming a sufficiently high frequency which is unaffected by ionospheric refractions. This frequency is greater than 1000MHz at day time and a few hundred MHz at night time. The resulting elevation and range measurement errors are then due to the tropospheric effects alone and are analysed for a normal, static, ductless, undisturbed atmosphere, based on monthly mean of refractivity for various places in India.

## 1.2 Radio Refractive Index of Air

Since radio energy at frequencies greater than 30 MHz is not normally reflected by ionosphere, the variation in the characteristics of the received fields is attributed to the variations in the lower atmosphere and in particular, to the variation of radio refractive index of troposphere. Electromagnetic waves travel in straight lines in free space, however, in the atmosphere, there is a normal downward bending of such

rays and is attributed to the normal decrease of refractive index,  $n$ , with height. Radar range and elevation angle errors are determined by the time delay and the bending of the radio ray, respectively, which are dependent on the refractive index. In view of this, it is necessary to evaluate refractive index of the medium in which the rays are travelling.

Refractive index can be measured directly or indirectly. The direct measurement is based on the relation  $n = \frac{C}{v}$ , where  $C$  is the velocity of light in vacuo, and  $v$  is the velocity of em waves in air,  $n$  is the refractive index. Radio frequency refractometers which are sensitive to the speed of propagation, are used for direct measurement, however these are complex and expensive and are not commonly used. Indirect method is based on the meteorological variables like water vapor pressure, air temperature and air pressure. Such methods are much simpler and are mostly used all over the world. In troposphere, the refractivity,  $N$ , at a given height  $h$ , is given by

$$N = (n-1) \times 10^6 = \frac{a}{T}(p + \frac{b}{T}e) \quad (1.1)$$

where,  $T$  is the air temperature in  $^{\circ}\text{K}$ ,  $p$  is the total atmospheric pressure in mbars and  $e$  is the partial pressure of water vapour in mbars at height  $h$  and  $a$  and  $b$  are constants. Most commonly used and CCIR recommended values of constants  $a$  and  $b$  are those given by Smith and Weintraub [2], which are  $77.7^{\circ}\text{K}/\text{mbar}$  and  $4810^{\circ}\text{K}$  respectively. These parameters are



available from weather service data and based on these,  $N$  values can be found for corresponding heights. As per Smith and Weintraub [2], equation (1.1) is independent of frequency in the 100 MHz to 10 GHz range and is valid upto 30 GHz with 0.5 percent accuracy in  $N$  units, and normal encountered ranges of temperature, pressure and humidity. These parameters can also be found accurately from atmospheric emission data by using radiative transfer equation [27] but the procedure is costly and complex and is not very popular.

### 1.3 Surface and Sea Level Refractivity

After  $N$  has been found for various heights, the next problem is to evaluate bending of the ray. Bending effects can be measured either by dividing the atmosphere into layers of varying thickness or by assigning a specific functional form to  $N$ , as discussed in next chapter. For these, the refractivity of ground  $N_S$ , at the place of measurement is essential. Kulshreshta and Chatterjee [3] have computed  $N_S$  values for India based on the five year averages of meteorological observations for 36 stations. Due to the dominating influence of the changes of density with height, the surface refractivity is dependent on the station altitude. This dependence has been eliminated by Venkiteshwaran et al [4] by reducing  $N_S$  to  $N_0$ , refractivity at sea level, and  $N_0$  charts have been prepared by them on monthly basis for whole of India. They have also enumerated the difference between formulae used for conversion of  $N_S$  to  $N_0$  for

Indian peninsula and that given for U.S.A. by Bean and Dutton [2], main difference being in the height of tropopause and in the definition of reference atmosphere.

#### 1.4 Reference Atmosphere

Dolukhanov [5] has given International standard atmosphere now often called standard troposphere as defined by International Commission for Aeronavigation as the one having the following characteristics

Sea level atmosphere pressure = 1013 mbars

Sea level temperature =  $15^{\circ}\text{C}$

Relative Humidity = 60 percent

It is also assumed that standard pressure lapse rate and standard temperature lapse rate are 0.12 mbar/meter and  $0.0055^{\circ}\text{C}/\text{meter}$  of height, respectively. Relative humidity is assumed constant at all heights. Standard troposphere extends upto 11 Kms. However, this is not applicable to Indian tropical climate. A standard atmosphere for tropics as mentioned by Srivastava [6] has following parameters

Mean sea level pressure = 1013.2 mbars

Mean sea level temperature =  $27^{\circ}\text{C}$

Lapse rate in temperature in the lowest 5 Kms is taken as  $0.0054^{\circ}\text{C}/\text{meter}$ . Tropopause for India [7] is 16 Kms during monsoons. Due to very large variation in relative humidity from place to place in tropics, the tropical standard

atmosphere defined above does not contain specifications of relative humidity and as pointed out by Venkateshwaran et al [4], the maximum error for converting  $N_S$  to  $N_0$  is not more than 3N units in any month over India, particularly so when station altitude above sea level does not exceed 500 meters.

### 1.5 Elevation Angle and Radar Range Errors

The elevation angle and range errors arise due to the refractive bending and the retardation of the velocity of propagation of em waves in atmosphere. These errors are known bias errors since their magnitudes are calculable. As per Nathanson [8], the uncertainties in their exact magnitudes, about 10 percent, from simplifying assumptions concerning the state of the atmosphere is partly from unknown bias errors and partly from rms inaccuracies. Calculations of these errors is generally based on averaged refractivity data, data from radio-sonde stations or on functional expressions of refractivity with respect to height. For the first technique as well as for the second technique, layer approach is used which requires a lot of refractivity data for innumerable stations for various heights. This data is insufficient for India. In functional approach general technique employed was to assume a refractivity model in which refractivity decreases linearly with height, called effective earth's radius model. However, as has been well documented [2], [9], this leads to errors at long ranges and low elevation angles for which accurate results are greatly

desired. Better results are obtained by using one or two term exponential models based on averaged refractivity values, which obviously have limited applicability for a specific time and location. Majumdar [10] has discussed a biexponential model for inland regions and a two part model consisting of a linear variation upto 1.5 Kms. followed by an exponential variation for coastal areas for India. However, Srivastava and Pathak [11],[12], have deduced exponential models for inland and coastal stations of India for CCIR recommended months of February, May, August and November, which corresponds to Winter, Summer, Monsoon and post-monsoon periods. However, these four months are unable to represent varying climatical conditions of tropical climate like that of India and as such Venkateshwaran et al[4] have taken monthly averages for various places in India for finding refractivity pattern. They have also found it reasonable to assume a negative exponential model for practical applications in India, and the same is used for finding radar measurement errors. The results are accurate for inland stations and given fairly good values for coastal stations of India.

Tropospheric conditions over Delhi were simulated on the computer by random generation of 1000 normally distributed  $N_s$  values by Monte-Carlo techniques by using known mean and standard deviation of average monthly  $N_s$  values. These are then used to find the elevation angle and range errors of a target for comparative study.

## CHAPTER II

DETERMINATION OF RADAR MEASUREMENT ERRORS2.1 Introduction

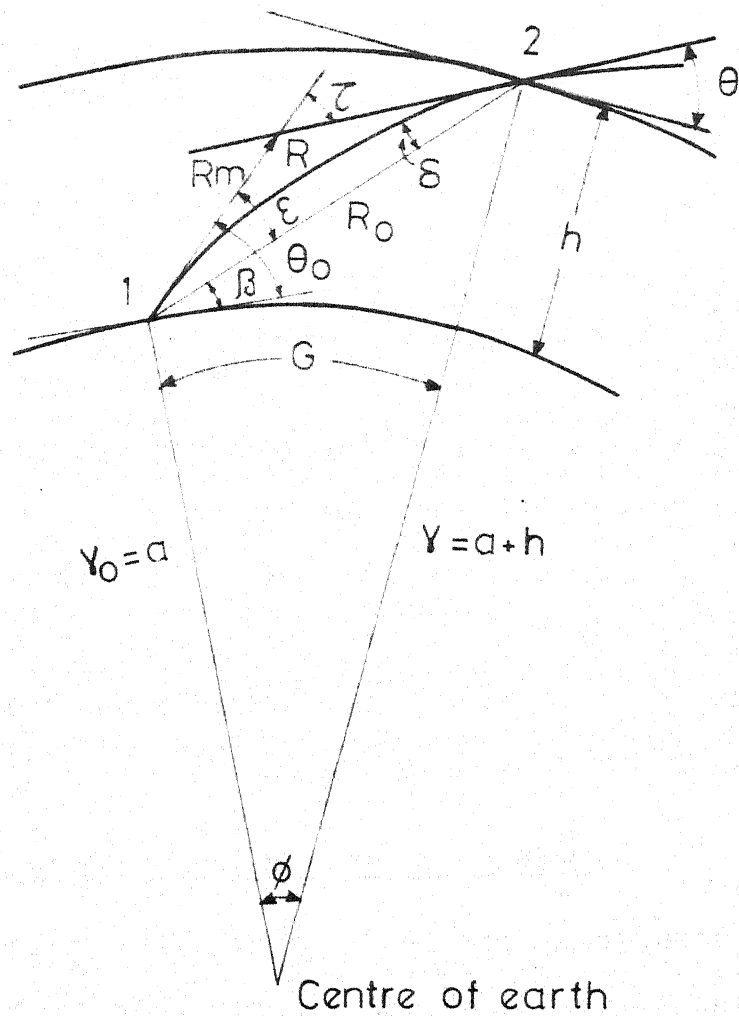
In general the data available to a radar from a target is the apparent elevation angle ( $\theta_0$ ) and apparent range (R), refer to Figure 2.1, whereas the desired parameters are the true elevation angle ( $\beta$ ) and the true slant range ( $R_0$ ). When an em wave propagates through the atmosphere, the wave undergoes a change of direction, or refractive bending according to Fermat's principle of least time which states that the path chosen by a ray joining two points is that path which can be traversed in the least possible time. This results in an error in the measurement of elevation angle of the target and is denoted as,

$$\epsilon = \theta_0 - \beta \quad (2.1)$$

The range error, which is the difference between the apparent and true range of the target arises due to (a) the increase in the path length due to the curvature of the ray path and (b) decreased propagation velocity in the atmosphere as compared to the free space velocity. In general (b) is less effective as compared to (a). The geometrical distance along the ray path is

$$R = \int_{r_0}^r \frac{1}{\sin \theta} dr \quad (2.2)$$

Whereas, the radio range or electrical distance along the ray



Legend:- (1) Origin of ray.

(2) Terminal point of ray.

Fig. 2.1 GEOMETRY OF THE REFRACTION OF THE em WAVE IN THE EARTH'S ATMOSPHERE.

path measured by the radar that assumes the wave propagation speed to be that of light is,

$$R_e = nR = \int_{r_0}^r \frac{n}{\sin \theta} dr \quad (2.3)$$

From equations (2.2) and (2.3) we get one way radar range error of the target

$$\Delta R = R_e - R_0 \quad (2.4)$$

Once the errors given by equations (2.1) and (2.4) are evaluated, true fix of a target can be obtained. However, the basic requirement is that of ray tracing and in the following sections, various techniques have been given for doing so. Also a number of representative methods for finding the errors are reviewed.

## 2.2 Tropospheric Refraction Effects on EM Waves

The geometry of the ray path in normal atmosphere is given in Figure 2.1, which also defines the variables of interest.  $\tau$ , the bending of the ray, is the total angular refraction of the ray path between two points. Refractive index,  $n$ , is slightly greater than unity near the earth's surface and approaches unity with increasing height. Assuming that refractive index is a function only of height above the surface of a smooth, spherical earth, i.e. it is horizontally homogeneous, the path of radio rays obeys Snell's law for polar coordinates and is given by,

$$n_2 r_2 \cos \theta_2 = n_1 r_1 \cos \theta_1 \quad (2.5)$$

where subscripts '1' and '2' correspond to initial point and the final point of the ray path.  $\tau$ , as per Bean and Dutton [2] is given by,

$$\tau_{12} = - \int_{n_1}^{n_2} \cot \theta \frac{dn}{n} \quad (2.6)$$

where  $n_1$  and  $n_2$  are corresponding refractive indexes at points 1 and 2 and  $\theta$  is the elevation angle at final point of the ray path. However, ray tracing is subject to the following restrictions:

- (1) The refractive index should not change appreciably in a wave length, and
- (2) The fractional changes in the spacing between neighbouring rays, which are initially parallel, must be small in a wave length.

Condition (1) is violated in case of discontinuity in refractive index, which is usually rare, or if the gradient of refractive index,  $dn/dr$ , is very large, in which case condition (2) is also violated. In case of ducting both these conditions are violated. Bean and Dutton [2] have found out that ducts do not occur for altitudes greater than 3 Kms and for more than 15 percent of the total time, which has also been confirmed by Chatterjee [13] for various places in India. In addition to these restrictions, the requirement of horizontal homogeneity in order to derive equation (2.6) is not realized under actual atmospheric conditions. However, Bean and Dutton [2] have shown that this effect can be



ignored between sea level stations, which are at a distance of less than 500 Kms from each other and also horizontal variations are most effective along the surface of the earth, thus affecting only those rays which follow a path close to the earth's surface.

### 2.3 Evaluation of Ray Bending

$\tau_{12}$  as given by equation (2.6) cannot be evaluated easily and for solving it, two approaches have been followed; one is the approximation to the integral and the second is the approximation to the atmosphere. The first leads to functional approach and the second to layer approach. Based on these, following methods are generally employed

- (1) Schulkin's method
- (2) Effective earth's radius model
- (3) Modified effective earth's radius model
- (4) Exponential model
- (5) Initial gradient method
- (6) Departure from normal method
- (7) Regression analysis
- (8) Graphical method.

#### 2.3.1 Schulkin's method:

If N-profile is known extensively, then this method gives accurate values with an error less than 0.04 percent. The N-profile consists of a series of values of N for different heights and a linear variation is assumed between the tabulated points. The N versus height profile consists of a series of interconnected

linear segments, and equation (2.6) is then integrated over each segment, yielding the desired results. If in denominator of equation (2.6),  $n$  is dropped, which gives the abovementioned 0.04 percent error, then segmentwise integration yields

$$\begin{aligned}\Delta\tau_{1,2}(\text{rad}) &\approx - \int_{n_1}^{n_2} \cot \theta \, dn \\ &\approx \frac{2(n_1 - n_2)}{\tan \theta_1 + \tan \theta_2} \\ \text{or, } \Delta\tau_{1,2}(\text{mrad}) &\approx \frac{2(N_1 - N_2) \times 10^{-3}}{\tan \theta_1 + \tan \theta_2} \quad (2.7)\end{aligned}$$

which is a result having an accuracy much better than the desired value, so,  $\tan \theta$  is replaced by  $\theta$  for values of  $\theta$  less than  $10^\circ$ , resulting in an expression,

$$\Delta\tau_{12}(\text{mrad}) \approx \frac{2(N_1 - N_2)}{\theta_1 + \theta_2} \quad (2.8)$$

where now  $\theta_1, \theta_2$  are in mrad. This approximation introduces an additional error nearly equal to 1 percent. The bending for the whole profile is then

$$\tau_n(\text{mrad}) \approx \sum_{k=1}^n \frac{2(N_k - N_{k+1})}{\theta_k + \theta_{k+1}} \quad (2.9)$$

This is a very accurate method and other methods try to achieve its accuracy. Main drawback is that a vast amount of data is required which is not available in India.

### 2.3.2 Effective earth's radius model

This method is due to Schelleng, Burrows and Ferrell and takes the bending of the ray path into account by defining an effective earth's radius,  $a_e = ka$ , where  $a$  is true earth's radius and  $k \approx 4/3$ . The ray then assumes a straight path and various parameters of interest can be calculated easily. Equation (2.6) after removing  $n$ , and substituting  $dn/dh = -1/4a$  [2], becomes,

$$\tau_{12} = \int_{h_1}^{h_2} \frac{\cot \theta}{4a} dh \quad (2.10)$$

where  $\theta$  is determined from the relation

$$\theta_h = [\theta_o^2 + \frac{3}{2} \frac{h}{a}]^{\frac{1}{2}} \quad (2.11)$$

and for the case  $h_1 = h_o = 0$  and  $0 \leq \theta_o \leq 10^\circ$ , equation (2.10) is written as,

$$\tau_{oh} = \int_0^h \frac{dh}{4a\theta} \quad (2.12)$$

This model also gives radio horizon  $G_{oh}$  as,

$$G_{oh} = \sqrt{2kah} \quad (2.13)$$

and if  $G_{oh}$  is in miles,  $a$  in miles and  $h$  in feet, then equation (2.13) reduces to

$$G_{oh}(\text{miles}) = \sqrt{2h} \quad (2.14)$$

Here  $h$  is the antenna height.

Extensive amount of tables, graphs and maps of gradients of  $N$  that permit world wide estimation of the seasonal range of

k are available and from these radio horizon distance can be found out, and other parameters are calculated. However, it is well documented that this model does not give very good representation of actual atmospheric N-structure above a height of 1 Km.

### 2.3.3 Modified effective earth's radius model

The first term of equation (1.1) involving P/T comprises atleast 70 percent of the total value of N, and is proportional to air density, which is a well known exponential function of height, so one expects refractivity to decrease exponentially with height. Taking this into account the deficiency of effective earth's radius model can be reduced to some extent. Since the first term in the expression for refractivity (equation (1.1)) is proportional to air density, and the water vapor term is negligible at an altitude of 16 Km for India [7], the refractivity also tends to be constant at this altitude and is equal to 46N units. So, linear model is used upto 1 Km and N can be represented by exponential function from 1 to 16 Kms, giving the expressions

$$N(h) = N_S + (h - h_S)\Delta N \quad h_S \leq h \leq h_{S+1} \quad (2.15)$$

$$\text{and } N(h) = N_1 e^{C_e(h-h_{S+1})} \quad h_{S+1} \leq h \leq 16 \text{ Kms} \quad (2.16)$$

where  $\Delta N = N_S - N_1$  and its values are available for various Indian stations.

$$\text{Also, } C_e = \frac{1}{15-h_S} \ln \frac{N_1}{46} \quad (2.17)$$

where  $N_1$  is the value of  $N(h)$  at 1 Km altitude.

Above 16 Kms, where less than 10 percent of total bending occurs, a single exponential decrease of  $N$  can be assumed, as given by the expression [7],

$$N_h = 700 e^{-0.1701h} \quad h \geq 16 \text{ Km} \quad (2.18)$$

The three part model expressed by equations (2.15), (2.16) and (2.18) has the advantage of the effective earth's radius approach plus being in reasonably good agreement with the average  $N$  structure of the atmosphere.

#### 2.3.4 Exponential model

The next better approximation is the one in which a single distribution of  $N$  is assumed and this is called negative exponential model, where

$$N(h) = N_S e^{-C_e(h - h_S)} \quad (2.19)$$

$$\text{and} \quad C_e = \ln \frac{N_S}{N(1\text{Km})} = \ln \frac{N_S}{N_S - \Delta N} \quad (2.20)$$

Equations (2.19) and (2.20) are used to determine  $N$  at all heights. This model is a close representation of the average refractivity structure for all heights for most of the regions of the world. Further, this is an entirely continuous function and is extensively used in theoretical studies all over the world. However, data for a sufficient period of time should be available to find average  $N_S$  and  $\Delta N$  for better accuracies.

### 2.3.5 Initial gradient method

The effect of anomalous initial N-gradients on ray propagation at near zero elevation angles, and for gradients less than ducting i.e.,  $dN/dh > -157$  N units/Km, may be very large. This may give errors if exponential model is used. To avoid this error, the initial gradient method utilises both the initial value,  $N_S$ , and the initial height gradient,  $\delta N'$ , of the refractive index over first 100 meters above the earth's surface. Basically, it is assumed that exponential model is applicable for all heights, and most of the error is because of the difference of  $\delta N'$  from the value predicted by the exponential model. Total bending,  $\tau$ , at any height is given by

$$\tau_h(N_S, \theta_o) = \tau_{h, \exp}(N_S, \theta_o) + \delta \tau_{\exp}(\delta N', \theta_o) \quad (2.21)$$

In practice  $\delta N'$  is approximated by  $\delta N$ , where,

$$\delta N' = \left( \frac{dN}{dh} \right)_{h=h_S} \quad (2.22)$$

i.e.

$$-\delta N = \frac{N_S - N_h}{h - h_S} \quad (2.23)$$

Here, value of  $N_h$  is found either from the first level reported by the radio sonde above the surface or from tower or tethered balloon measurements, where  $h - h_S = 30$  to 300 meters. For further analysis, it is necessary to know what value of  $N_S$  the observed value of  $\delta N$  will correspond to in the exponential reference atmosphere, denoting it by  $N_S^*$  and using equations (2.19) and (2.23), we get

$$-\delta_N = \frac{N_S^* - N_S^* e^{-C_e^*(h-h_S)}}{h - h_S} \quad (2.24)$$

or

$$N_S^* = \frac{-\delta_N(h - h_S)}{1 - e^{-C_e^*(h-h_S)}} = \frac{-0.1 \delta_N}{1 - e^{-0.1 C_e^*}} \quad (2.25)$$

In practice, it is more convenient to use the graphical relation between  $N_S^*$  and  $\delta_N$  and find the additive correction factor which is the simple difference between the values of 100 meter layer bending as determined by  $N_S$  and  $N_S^*$ , i.e.

$$\delta T_{\text{exp}}(\delta N', \theta_o) = \tau_{\text{exp},0.1}(N_S^*, \theta_o) - \tau_{\text{exp},0.1}(N_S, \theta_o) \quad (2.26)$$

and using this equation, equation (2.21) reduces to

$$\tau_h(N_S, \theta_o) = \tau_{h,\text{exp}}(N_S, \theta_o) + \tau_{\text{exp},0.1}(N_S^*, \theta_o) - \tau_{\text{exp},0.1}(N_S, \theta_o) \quad (2.27)$$

It is claimed that this method is very useful as compared to exponential model for initial elevation angles of less than 10 mrad and upto a total height of 70 Kms. This method also predicts any possible trapping of the ray.

### 2.3.6 Departure from normal method

This method calculates bending by two ways, one by assuming exponential model and second by the observed  $N(h)$  profile; and is primarily intended for pointing out the difference between the actual ray bending and the average ray bending that is predicted by the exponential  $N(h)$  profile. An A unit is

defined to study the difference between the two, and is expressed as,

$$A(N_S, h) = N(h) + N_S(1 - e^{-C_e h}) \quad (2.28)$$

From this  $\delta A(N_S, h)$  is evaluated, which is a measure of the departure of  $N(h)$  from the normal exponential profile and is expressed as

$$\begin{aligned} \delta A(N_S, h) &= A(N_S, h) - N_S \\ &= N(h) - N_S e^{-C_e h} \end{aligned} \quad (2.29)$$

If equation (2.28) is differentiated and substituted in equation (2.6), value of  $\tau_{o,h}$  obtained is,

$$\begin{aligned} \tau_{o,h} &= \tau_{N_S}(h) + \sum_{k=0}^{k_h} - \frac{2}{\theta_k + \theta_{k+1}} [\Delta A(N_S)]_{N_k}^{N_{k+1}} \times 10^{-6} \\ (\text{rad.}) \quad (\text{rad.}) &\quad (\text{rad.}) \quad (\text{rad.}) \end{aligned} \quad (2.30)$$

where

$$\begin{aligned} \Delta A(N_S) &= \Delta N(h) + \Delta [N_S(1 - e^{-C_e h})] \\ &= \Delta N(h) + N_S C_e e^{-C_e h} \Delta h \end{aligned} \quad (2.31)$$

and  $\tau_{N_S}(h)$  is the tabulated value of  $\tau$  for various atmospheres.  $\theta_k$  and  $\theta_{k+1}$  are from the  $N_S$  exponential atmosphere. This model has the same limitations as Schulkin's method for its applicability to India.



### 2.3.7 Regression analysis

This statistical linear regression technique has been developed by Bean, Cahoon and Thayer. Here

$$\tau_{12} = a + b N_S \quad (2.32)$$

where  $a$  and  $b$  are constants and can be found by standard statistical linear regression methods, provided, large number of observed  $\tau_{12}$  for various  $N_S$  values for many values of  $h$  and  $\theta_0$  are available. Based on these observations, tables for  $a, b$  and standard errors of estimates of  $\tau_{12}$  for various heights can be made, and from these, bendings for other heights can be found out for any  $N_S$  values. Such data are also not available for India.

### 2.3.8 Graphical method

This method is due to Weisbrod and Anderson and is very handy for computing refraction in troposphere. This is similar to Schulkin's method, however, one difference being that small angle approximation is not taken into consideration while arriving at the results. From equation (2.7), total bending  $\tau$  is then given by

$$\tau(\text{mrad}) = \sum_{k=0}^n \frac{N_k - N_{k+1}}{500(\tan \theta_k + \tan \theta_{k+1})} \quad (2.33)$$

Terms for the denominator are determined from curves which are given by Weisbrod and Anderson [2]. However, this data is not available for India.

## 2.4 Methods for determining elevation and Range errors

There are various methods available in literature for finding these two errors. These errors can be calculated by ray tracing methods [14], or by numerical integration [15]. Formulae which are simpler and faster have also been published, but the necessary simplification has been obtained either by assuming an exponential profile with approximations [16] or by neglecting path curvature [17], or both [18]. Marini [19] has given a procedure to find errors in the rapid processing of satellite tracking data and this method gives accurate results, provided the satellite facilities are available. Berkowitz [20] has given details about various errors and has also given integrated and stratified layer methods for calculating these errors. A two quartic refractivity profile for predicting range error, particularly of satellites, is given by Hopfield [21].

Besides, measuring the true range and the true elevation angle of the target, it is also essential in certain radar applications [22], such as air traffic control or vectoring of fighters for intercepting the bombers, to know the accurate height of the target. Vogler [23] has given a method for determination of height of the target and error associated with it. Blake [15] has given an exhaustive method which determines true height, ground range, elevation error and range error of the target. This method is described in next chapter and is used for finding errors for various places in India.

## CHAPTER III

A COMPUTER PROGRAM FOR ERROR CALCULATION3.1 Introduction

A numerical method has been used for error calculations and it is designed for automatic operation over a wide range of elevation angles while retaining computational precision. The main features of this methods are

- (1) No approximations are made in the integrand.
- (2) The step size employed in the integration is varied automatically by an adaptive integration subroutine that uses Simpson's rule.
- (3) Special computations are carried out for the grazing ray at low altitudes.

Refer Figure 2.1, starting at an initial angle  $\theta_0$ , the integration is performed to altitude  $h$  to determine both the ground range  $G$  and the radio range  $R_e$  (hereafter denoted as  $R$ ), along the curved ray path. Levine etal [24] have combined the integrating expressions for  $G$  and  $R$ . Thayer [14] has employed a layer concept with a power law approximating function. However, due to paucity of data of  $N(h)$  profile for various places in India, a continuous nonlinear index profile, namely, negative exponential profile is used here and it is felt that under such circumstances Blake's [15] method is direct and simpler.

### 3.2 A Numerical Integration Method

This method calculates height  $h$  of the target, when  $\theta_0$  and  $R$  are available. Once, height is found; ground range  $G$ , true range  $R_0$ , elevation angle and range errors can be calculated. Using equation (2.5) and expressing  $\theta_2$  by  $\theta$ , and  $\theta_1$  by  $\theta_0$ , the expression is reduced to

$$\cos \theta = \frac{n_0 r_0 \cos \theta_0}{nr} \quad (3.1)$$

From Figure 2.1, as  $r = r_0 + h$ , equation (3.1) reduces to,

$$\cos \theta = \frac{n_0 \cos \theta_0}{n(1 + \frac{h}{r_0})} \quad (3.2)$$

where  $h$  is the ray height above the sea level. Snell's law leads to a ray tracing integral which allows computation of ray path length  $R_1$ , if the ray terminal height  $h_1$  and initial elevation angle  $\theta_0$  are given, i.e.  $R_1 = R(h_1, \theta_0)$ . However, this function cannot be integrated analytically and as such numerical methods are employed. The inverse problem of finding  $h_1$ , given  $R_1$  and  $\theta_0$ , i.e.  $h_1 = h(R_1, \theta_0)$ , is more difficult since the ray tracing equation cannot be explicitly expressed in this functional form. Blake [15] has developed a highly precise method for finding  $h_1$  by using a negative exponential refractivity profile and performing numerical integration of the entire ray tracing integrand. Refractive index for ionosphere is assumed to be unity with the result that there is no bending of ray in ionosphere. Marini [19] states that almost all the radio ray bending caused by the non-ionized atmosphere of the earth takes place within 70 Kms

altitude, so exponential profile is assumed to be applicable upto this altitude only, and after this  $n$  is taken as unity. This method is exact and its accuracy is limited in machine computation by the number of significant figures carried by the computer.

### 3.2.1 Ray tracing method

Refer Figure 2.1, taking small increments of  $dR$  and  $dh$  and assuming local elevation angle as  $\theta$ ,

$$\sin \theta = \frac{dh}{dR(\text{geometrical})} = \frac{ndh}{dR}$$

$$\text{or } dR = \frac{ndh}{\sin \theta} = \frac{ndh}{\sqrt{1 - \cos^2 \theta}} \quad (3.3)$$

Using equation (3.2) in equation (3.3) and integrating,

$$R(h_1, \theta_0) = \int_0^{h_1} \frac{ndh}{\sqrt{1 - \left( \frac{n_0 \cos \theta_0}{n(1 + \frac{h}{r_0})} \right)^2}} \quad (3.4)$$

Similarly, ground range,  $G$ , measured along earth's surface at sea level is

$$G(h_1, \theta_0) = \int_0^{h_1} \frac{dh}{\left(1 + \frac{h}{r_0}\right) \sqrt{\left( \frac{n(1 + h/r_0)}{n_0 \cos \theta_0} \right)^2 - 1}} \quad (3.5)$$

Taking spherical geometry and using law of Cosines, slant range  $R_0$  and true elevation angle  $\beta$  are given by

$$R_0 = \sqrt{h_1^2 + 4r_0(r_0 + h_1) \sin\left(\frac{G}{2r_0}\right)} \quad (3.6)$$

$$\sin \beta = \left[ \frac{h_1}{R_o} + \frac{h_1^2}{2r_o R_o} - \frac{R_o}{2r_o} \right] \quad \text{for } \theta_o \leq \frac{\pi}{4} \quad (3.7)$$

and

$$\cos \beta = \left[ \frac{(r_o + h_1) \sin(G/r_o)}{R_o} \right] \quad \text{for } \theta_o > \frac{\pi}{4} \quad (3.8)$$

The negative exponential profile used is,

$$N(h) = N_s e^{-C_e(h-h_s)} \quad (3.9)$$

where  $h$  is the height w.r.t. sea level. Further expanding equation (3.9)

$$\begin{aligned} N(h) &= N_s e^{C_e h_s} e^{-C_e h} \\ &= N_o e^{-C_e h} \end{aligned} \quad (3.10)$$

where  $N_o$  is the sea level refractivity of the station and  $C_e$  is the decaying constant. Antenna height is ignored here as it does not cause any significant error in the results.  $N_o$  and  $C_e$  values are taken from Kulshreshta and Chatterjee [3] and RTRC monograph No. 1.[4].

### 3.2.2 Height finding method

Next step is to find the height of the terminal point of ray given  $R$  and  $\theta_o$ , and this requires inversion of equation (3.4). Height is thus obtained by using an adaptive integration subroutine that uses Simpson's rule and the step size is varied automatically. Initial step computes  $R_{11}$  corresponding to  $h_{11}$

and for this, height of unrefracted ray,  $h_{\max}$ , is given by

$$h_{\max} = \sqrt{(a^2 + R^2 + 2aR \sin \theta_0)} - a \quad (3.11)$$

where  $r_0$  is replaced by  $a$ , the true radius of the earth as in Figure 2.1. Then a value  $h_{\min}$  is computed, which is the height of the ray in an atmosphere whose gradient is linear, and of a value equal to that of the earth's surface gradient of the actual atmosphere. Taking effective earth's radius  $a_e$  [2] as,

$$a_e = a \left[ \frac{1}{1 - \frac{C_e a \rho_0}{1 + \rho_0}} \right] \quad (3.12)$$

where  $\rho_0 = N_0 \times 10^{-6}$  and writing

$$h_{\min} = \sqrt{(a_e^2 + R^2 + 2a_e R \sin \theta_0)} - a_e \quad (3.13)$$

From equations (3.11) and (3.13), the first trial height  $h_{11}$  then is

$$h_{11} = \frac{h_{\max} + h_{\min}}{2} \quad (3.14)$$

Taking this  $h_{11}$ ,  $R_{11}$  is found from equation (3.4) and compared with desired  $R_1$ . If  $R_1 > R_{11}$ , second trial value of  $h_1$  is  $h_{12}$ , where

$$h_{12} = h_{11} \pm \frac{(h_{\max} - h_{\min})}{4} \quad (3.15)$$

Again, second tentative value of  $R_1$ ;  $R_{12}$ , is found from equation (3.4). Iterations are then carried out as per the formula

$$h_{1n} = \frac{(R_1 - R_{1(n-1)})(h_{1(n-2)} - h_{1(n-1)})}{(R_{1(n-2)} - R_{1(n-1)})} + h_{1(n-1)} \quad (3.16)$$

and range  $R_{1n}$  is found successively. The process is continued till the difference between  $R_{1n}$  and  $R_1$  is equal to the desired value. Newton's method for comparing these two values is employed, and a quantity  $T$ , where

$$T = \frac{R_{1n} - R_1}{R_1} \quad (3.17)$$

is compared with the number  $10^{-N}$ , where  $N(=6)$  is the number of significant figures to which the agreement is desired. When  $T \leq 10^{-N}$ , the process is terminated. The height  $h_{1n}$  is then the desired height at range  $R = R_1$ . This value of  $h_{1n}$  is then used to find ground range  $G$  from equation (3.5) and  $R_0$  and  $\beta$  from equations (3.6) to (3.8). Finally, elevation angle error is found from equation (2.1) and one way radar range error is found from equation (2.4). It is found out that for one value of  $\theta_0$  and 20 values of range  $R$ , the computational time required is

9 sec on IBM 7044. By punching 'DECK' in Column 16 of IBFTC card, the whole program was converted into binary deck and this saved 1 mt 52 sec of compilation time of the program by the computer.

As equations involved for precise numerical computation should avoid formulations that destroy the accuracy by taking the difference of two nearly equal numbers, which happens to be the case with equations (3.4) and (3.5) at small elevation angles and near zero heights, so these have to be manipulated into a



better form for accurate computation. This procedure is followed here. Replacing  $\cos \theta_0$  by  $\sqrt{1 - \sin^2 \theta_0}$  and assuming,  $n = 1 + N_0 \times 10^{-6} e^{-C_e h}$  and  $\rho_0 = N_0 \times 10^{-6}$ , we get from equations (3.4) and (3.5), the following better expressions,

$$R(h_1, \theta_0) = \int_0^{h_1} \frac{n^2(1 + \frac{h}{a})}{\sqrt{(u+V+W+VW)}} dh \quad (3.18)$$

and

$$G(h_1, \theta_0) = \int_0^{h_1} \frac{(1 + \rho_0) (\cos \theta_0) dh}{(1 + \frac{h}{a}) \times \sqrt{(u+V+W+V.W)}} \quad (3.19)$$

where

$$n = 1 + \rho_0 e^{-C_e h}$$

$$u = (1 + \rho_0)^2 \sin^2 \theta_0 - 2\rho_0 - \rho_0^2$$

$$V = 2\rho_0 e^{-C_e h} + \rho_0^2 e^{-2C_e h}$$

$$W = \frac{2h}{a} + \frac{h^2}{a^2}$$

In the regions close to  $\theta_0 = 0^\circ$  and  $h = 0$ , equations (3.4) and (3.5) become infinite and as such numerical integration is impossible, so some special procedure has to be adopted to overcome this problem.

### 3.2.3 Special procedure for low angles and heights

For  $\theta_0 = 0^\circ$  and  $h = 0$ , the radicands in the denominator of the integrands in equations (3.4) and (3.5) are approximated by Taylor's series upto terms of second degree, giving a general

expression of the form

$$F(h_1) = A \int_0^{h_1} \frac{dh}{\sqrt{(bh^2 + Ch + d)}} \quad (3.20)$$

where F represents either R or G and A, b, C, d will have values corresponding to these and are denoted as  $A_R$ ,  $b_R$ ,  $C_R$ ,  $d_R$  and  $A_G$ ,  $b_G$ ,  $C_G$ , and  $d_G$ . From integration tables, equation (3.20) is written as

$$F(h_1) = \frac{A}{\sqrt{b}} \ln \left[ \frac{2bh_1 + C + 2\sqrt{b(bh_1^2 + Ch_1 + d)}}{C + 2\sqrt{bd}} \right] \quad (3.21)$$

For better computational precision,  $\cos^2 \theta_0$  is taken as  $= 1 - \sin^2 \theta_0$  for  $\theta_0$  near  $0^\circ$ . And the constants are expressed as,

$$A_R = 1 + \rho_0$$

$$b_R = C_e \gamma - \gamma^2 + \frac{8\gamma}{a} - \frac{3}{a^2} + \sin^2 \theta_0 [10\gamma^2 - \frac{8\gamma}{a} - 2C_e \gamma + \frac{3}{a^2}]$$

$$C_R = 2[(2\gamma - \frac{1}{a})\sin^2 \theta_0 - \gamma + \frac{1}{a}]$$

$$d_R = d_G = \sin^2 \theta_0$$

$$A_G = \cos \theta_0$$

$$b_G = C_e \gamma + \gamma^2 - \frac{8\gamma}{a} + \frac{5 + \sin^2 \theta_0}{a^2}$$

$$C_G = 2\left[\frac{1 + \sin^2 \theta_0}{a} - \gamma\right]$$

where  $\gamma$  is a parameter given by

$$\gamma = \frac{\rho_0 C_e}{1 + \rho_0} \quad (3.22)$$

and as  $a_e = \frac{a}{1 - \gamma a}$  for effective earth's radius model,  $\gamma$  can also be expressed as,  $\gamma = \frac{1}{a} - \frac{1}{a_e}$ .

The argument of  $\ln$  expression in equation (3.21) is very slightly greater than unity for small values of  $h_1$ , so, for computational precision, it is expressed in the form,

$$F(h_1) = \frac{A}{\sqrt{b}} [\ln(1 + x)]$$

where

$$x = \frac{2bh_1 - 2\sqrt{(bd)} + 2\sqrt{(b(bh_1^2 + Ch_1 + d))}}{C + 2\sqrt{(bd)}} \quad (3.23)$$

The value of  $\ln(1+x)$  is programmed for computer evaluation to eight significant figures by the use of the series

$$\ln(1 + x) = x - \frac{x^2}{2} + \frac{x^3}{3} \quad (3.24)$$

These approximations are used for height interval from  $h = 0$  to  $h = 1$  meter and for  $\theta_0$  upto  $1^\circ$ .

### 3.3 The Computational Method

Ray tracing required in the height finding computation is done in a piecewise fashion in order to avoid Simpson's rule integration of a single large height interval. The integration is done from  $h = 0$  or  $h = 1$  meter (depending on whether  $\theta_0$  is or is not greater than  $1^\circ$ ) to  $h = 10$  meters in 1-meter step and from  $h = 10$  meters to  $h = 100$  meters in 10 meter step. The interval from  $h = 100$  to  $h = 70,000$  meters is integrated in two steps, the first from  $h = 100$  to  $h = 5,000$  meters and the second from  $h = 5,000$  meters to  $h = 70,000$  meters (or to the specified height if it is less than these values). From  $h = 0$  to 1 meter and  $\theta_0$  less than  $1^\circ$ , approximations as given in para (3.2.3) are used.

For  $h$  greater than 70 Kms, the assumption  $n(h) = 1$  is made and the ray follows a straight line path. In this case, height is found geometrically. The radar range and ground range corresponding to the height increment from  $h_C$  ( $= 70$  Kms) to the height of terminal point  $h_1$  is denoted by DR and DG.  $D\phi$  is the corresponding increment of angle  $\phi$ . The local elevation angle  $\theta_C$  (corresponding to  $\theta(h_C)$ ) is found from equation (2.5),

$$\cos \theta_C = \frac{(1 + \rho_o) \cos \theta_o}{(1 + \frac{h_C}{a})(1 + \rho_o e^{-C e^{h_C}})} \quad (3.25)$$

and as at height  $= h_C$ ,  $n(h_C) = 1$ , the equation (3.25) is written as

$$\cos \theta_C = \frac{(1 + \rho_o) \cos \theta_o}{(1 + \frac{h_C}{a})} \quad (3.26)$$

The height  $h_1$ , is then, from the law of cosines

$$h = \sqrt{[(h_C + a)^2 + (DR)^2 + 2(h_C + a)(DR) \sin \theta_C]} - a \quad (3.27)$$

where  $DR = R_1 - R(h_C)$

$DG = a \tan(D\phi) = a d\phi$ , for low angles

where, from (3.25) and law of sines,

$$\sin D\phi = \frac{(1 + \rho_o) (\cos \theta_o) (DR)}{(1 + \frac{h_C}{a}) (a + h_1)} \quad (3.28)$$

All quantities are known and  $\Delta R$  and  $\epsilon$  can be found for any range and elevation angle.

The Fortran program is given in Appendix A and has been used for calculation of various parameters as given in next chapter for different places of India.

## CHAPTER IV

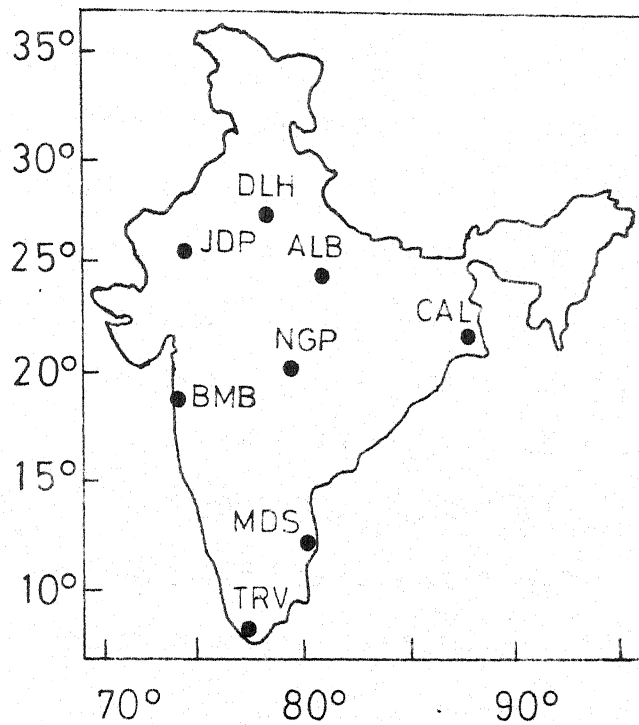
CALCULATIONS AND RESULTS4.1 Introduction

Computer program developed in last chapter has been used to find the true range, ground range, true elevation angle, height, elevation angle and range errors of the target for eight places in India, namely, New Delhi, Allahabad, Nagpur, Jodhpur, Calcutta, Bombay, Madras and Trivandrum for all the months and the yearly mean, based on average monthly  $N_0$  and  $C_e$  data given by Venketashwaran et al [4]. These places are indicated in Figure 4.1 along with their altitude above sea level and the type of climate. It is assumed that the input quantities which are available are the apparent range,  $R$ , and the apparent elevation angle,  $\theta_0$ , of the target.

Although the computer program is suitable for any range from 0 to infinity and any elevation angle from  $0^\circ$  to  $90^\circ$ , the actual values taken for range vary from 10 Kms to 600 Kms, and for elevation angle from  $0.5^\circ$  to  $75^\circ$ . Minimum range is fixed due to computer limitations and max. range is fixed on the basis of present day radar systems available in the country. Limiting values of elevation angle are fixed due to the limitations of the computer.

4.2 Tables for Radar Measurement Errors

As indicated in Figure 4.1, the eight selected places are classified into three climatic groups. It was also found by



Place	Symbol	Altitude above sea level (MRS)	Climatic pattern
Delhi	DLH	216	Continental
Allahabad	ALB	98	"
Nagpur	NGP	310	"
Jodhpur	JDP	224	"
Calcutta	CAL	6	Subtropical
Bombay	BMB	15	"
Madras	MDS	6	Tropical
Trivandrum	TRV	8	"

Fig. 4.1 RADIOSONDE STATION LOCATION MAP AND CLIMATIC PATTERN.

observation of elevation angle and range error values that errors follow similar general pattern and are also nearly alike for places under each group. Accordingly a representative location from each group has been selected for further analysis and these are, Delhi, Madras and Calcutta. Calculated values of various parameters for these places which are based on yearly mean values of  $N_0$  and  $C_e$  are given in Tables 4.1 to 4.3 for elevation angles of  $0.5^\circ$ ,  $5^\circ$ ,  $30^\circ$  and  $75^\circ$ . Table 4.4 is a consolidated table which gives variation limits of maximum range and elevation angle errors along with their mean values for typical range of 300 Kms and elevation angle of  $0.5^\circ$ . This table also gives  $N_0$  variations and yearly mean  $N_0$  limits. Correspondence of error values with  $N_0$  values for typical climatic pattern is found to be true for all ranges and angles.

#### 4.3 Error Curves

On analysis of the results, it is also observed that maximum errors occur for lowest value of elevation angle, namely  $0.5^\circ$ , and these carry on decreasing as the elevation angle increases. Also, for typical value of the elevation angle, errors increase with increase in range and this is particularly noticeable for low angle values. A typical range of 300 Kms was selected corresponding to average detection range of radar systems in the country and histograms of maximum range and elevation angle <sup>errors</sup> were drawn for all the 12 months for these eight places. Figures 4.2 to 4.9 consist of these histograms.  $N_0$  histograms based on average monthly values of  $N_0$  are also drawn for each place. It

Table 4.1: Table of ground range, height, elevation angle and range errors versus range of a target for Delhi for yearly mean  $N_0$  Value.

RADAR RANGE (KMS)	GROUND RANGE (KMS)	HMILES (KMS)	RANGE ERROR (MRS)	ELEVATION ERROR (DEGREES)
<u>ELEV = 0.5°</u>				
10	9.996	0.090	3.4	0.010
20	19.992	0.199	6.7	0.019
30	29.998	0.317	10.0	0.029
40	39.983	0.443	13.3	0.038
50	49.978	0.580	16.6	0.048
60	59.972	0.746	19.7	0.057
70	69.967	0.914	22.9	0.066
80	79.968	1.094	25.9	0.076
90	89.954	1.280	29.0	0.085
100	99.976	1.493	32.0	0.094
150	149.968	2.713	45.9	0.137
200	199.838	4.263	58.0	0.177
250	249.752	6.148	68.4	0.213
300	299.377	8.378	76.9	0.247
350	349.438	10.952	83.7	0.276
400	399.299	13.906	89.0	0.303
450	449.068	17.223	92.9	0.326
500	498.779	20.911	95.7	0.346
550	548.431	24.978	97.7	0.364
600	598.020	29.483	99.1	0.380
<u>ELEV = 5.0°</u>				
10	9.957	0.877	3.3	0.009
20	19.913	1.767	6.2	0.018
30	29.866	2.670	9.0	0.027
40	39.818	3.586	11.4	0.035
50	49.766	4.518	13.7	0.042
60	59.710	5.477	15.8	0.049
70	69.673	6.413	17.7	0.056
80	79.534	7.332	19.4	0.062
90	89.521	8.366	20.9	0.068
100	99.468	9.368	22.3	0.073
150	149.027	14.567	27.6	0.097
200	198.621	20.137	30.7	0.114
250	248.112	26.032	32.4	0.127
300	297.483	32.406	33.4	0.137
350	346.785	39.109	33.9	0.145
400	395.921	46.104	34.1	0.151
450	444.972	53.659	34.3	0.156
500	493.935	61.502	34.3	0.159
550	542.722	69.728	34.4	0.163
600	591.423	78.327	34.4	0.165

Continued.



ELEV = 30.0°

10.	8.672	5.009	2.7	0.007
20	17.292	10.018	4.3	0.012
30	25.919	15.042	5.3	0.016
40	34.537	20.079	5.9	0.019
50	43.125	25.127	6.2	0.021
60	51.724	30.197	6.5	0.023
70	60.298	35.238	6.6	0.024
80	68.859	40.340	6.7	0.025
90	77.407	45.437	6.7	0.026
100	85.961	50.540	6.7	0.027
150	128.489	76.240	6.8	0.029
200	170.527	102.233	6.8	0.030
250	212.327	128.432	6.8	0.031
300	253.777	155.030	6.8	0.031
350	294.890	181.845	6.8	0.032
400	335.671	208.932	6.8	0.032
450	376.112	236.235	6.8	0.032
500	416.220	263.905	6.8	0.032
550	455.992	291.721	6.8	0.032
600	495.433	319.916	6.8	0.032

ELEV = 75.0°

10	2.534	9.650	2.2	0.002
20	5.161	19.317	3.0	0.003
30	7.750	28.979	3.3	0.004
40	10.292	38.641	3.4	0.004
50	12.846	48.385	3.5	0.004
60	15.393	57.970	3.5	0.004
70	17.931	67.635	3.5	0.004
80	20.463	77.302	3.5	0.005
90	22.936	86.970	3.5	0.005
100	25.592	96.639	3.5	0.005
150	37.971	144.998	3.6	0.005
200	50.255	193.381	3.6	0.005
250	62.368	241.789	3.6	0.005
300	74.289	290.220	3.6	0.005
350	86.046	338.674	3.6	0.005
400	97.624	387.151	3.6	0.005
450	109.057	435.650	3.6	0.005
500	120.310	484.170	3.6	0.005
550	131.422	532.711	3.6	0.005
600	142.370	581.273	3.6	0.005

Table 4.2: Table of ground range, height, elevation angle and range errors versus range of a target for Madras for yearly mean  $N_0$  value.

RADAR RANGE (KMS)	GROUND RANGE (KMS)	HMILES (KMS)	RANGE ERROR (MRS)	ELEVATION ERROR (DEGREES)
<u>ELEV=0.5°</u>				
10	9.996	0.093	3.7	0.010
20	19.991	0.199	7.3	0.020
30	29.987	0.317	10.9	0.030
40	39.982	0.447	14.5	0.039
50	49.976	0.589	18.0	0.049
60	59.971	0.744	21.5	0.059
70	69.965	0.912	24.9	0.068
80	79.958	1.091	28.3	0.078
90	89.951	1.284	31.6	0.087
100	99.943	1.489	34.9	0.096
150	149.897	2.704	50.2	0.141
200	199.833	4.244	63.8	0.182
250	249.746	6.117	75.4	0.220
300	299.631	8.332	85.1	0.255
350	349.483	10.899	92.9	0.287
400	399.294	13.825	99.1	0.315
450	499.061	17.117	103.8	0.340
500	498.776	20.780	107.2	0.361
550	548.433	24.821	109.7	0.381
600	598.025	29.241	111.4	0.397
<u>ELEV = 5.0°</u>				
10	9.957	0.877	3.6	0.010
20	19.912	1.767	6.8	0.019
30	29.865	2.669	9.8	0.027
40	39.815	3.585	12.6	0.036
50	49.763	4.513	15.1	0.043
60	59.709	5.455	17.4	0.051
70	69.652	6.410	19.5	0.058
80	79.592	7.379	21.5	0.064
90	89.529	8.361	23.3	0.070
100	99.464	9.358	24.9	0.076
150	149.094	14.555	31.0	0.101
200	198.646	20.116	34.7	0.120
250	248.111	26.050	36.9	0.134
300	297.484	32.362	38.1	0.145
350	346.758	39.053	38.8	0.154
400	395.926	46.124	39.1	0.161
450	444.984	53.576	39.3	0.166
500	493.926	61.406	39.4	0.171
550	542.745	69.616	39.5	0.174
600	591.438	78.202	39.5	0.177

Continued.

ELEV = 30.0°

10	8.652	5.003	3.0	0.007
20	17.291	10.017	4.8	0.013
30	25.919	15.042	5.9	0.017
40	34.534	20.078	6.7	0.020
50	43.135	25.126	7.1	0.023
60	51.724	30.185	7.4	0.024
70	60.298	35.256	7.5	0.026
80	68.860	40.338	7.7	0.027
90	77.408	45.431	7.7	0.028
100	85.942	50.537	7.8	0.029
150	128.411	76.234	7.8	0.031
200	170.541	102.216	7.8	0.033
250	212.332	128.478	7.8	0.033
300	253.785	155.018	7.8	0.034
350	294.901	181.831	7.8	0.034
400	335.680	208.915	7.8	0.035
450	376.124	236.267	7.8	0.035
500	416.232	263.882	7.8	0.035
550	456.006	291.758	7.8	0.035
600	495.448	319.892	7.8	0.035

ELEV = 75.0°

10	2.584	9.657	2.4	0.002
20	5.161	19.317	3.4	0.003
30	7.730	28.978	3.8	0.004
40	10.292	38.641	4.0	0.004
50	12.846	48.304	4.0	0.004
60	15.393	57.969	4.1	0.005
70	17.932	67.635	4.1	0.005
80	20.463	77.302	4.1	0.005
90	22.987	86.969	4.1	0.005
100	25.503	96.638	4.1	0.005
150	37.971	144.997	4.1	0.005
200	50.256	193.380	4.1	0.005
250	62.362	241.788	4.1	0.005
300	74.291	290.219	4.1	0.005
350	86.048	338.673	4.1	0.005
400	97.637	387.150	4.1	0.006
450	109.060	435.648	4.1	0.006
500	120.322	484.168	4.1	0.006
550	131.425	532.710	4.1	0.006
600	142.374	581.272	4.1	0.006

Table 4.3: Table of ground range, height, elevation angle and range errors versus range of a target for Calcutta for yearly mean  $N_0$  value.

RADAR RANGE (KMS)	GROUND RANGE (KMS)	HMILES (KMS)	RANGE ERROR (MRS)	ELEVATION ERROR (DEGREES)
ELEV = $0.5^\circ$				
10	9.996	0.093	3.6	0.010
20	19.992	0.199	7.2	0.020
30	29.987	0.317	10.7	0.030
40	39.982	0.447	14.2	0.039
50	49.977	0.589	17.7	0.049
60	59.971	0.744	21.1	0.059
70	69.965	0.912	24.5	0.068
80	79.959	1.091	27.8	0.078
90	89.952	1.284	31.0	0.087
100	99.944	1.489	34.2	0.096
150	149.898	2.704	49.2	0.141
200	199.834	4.245	62.4	0.182
250	249.748	6.118	73.7	0.220
300	299.633	8.335	83.1	0.255
350	349.485	10.904	90.6	0.286
400	399.297	13.832	96.5	0.314
450	449.063	17.127	101.0	0.338
500	498.777	20.795	104.3	0.360
550	548.434	24.839	106.6	0.379
600	598.026	29.264	108.3	0.395
ELEV = $5.0^\circ$				
10	9.957	0.877	3.5	0.010
20	19.912	1.767	6.7	0.019
30	29.865	2.670	9.6	0.027
40	39.816	3.585	12.3	0.036
50	49.764	4.513	14.8	0.043
60	59.709	5.455	17.0	0.051
70	69.652	6.410	19.1	0.058
80	79.592	7.379	21.0	0.064
90	89.530	8.362	22.7	0.070
100	99.465	9.359	24.2	0.076
150	149.095	14.556	30.1	0.101
200	198.646	20.119	33.6	0.119
250	248.112	26.056	35.6	0.133
300	297.484	32.370	36.7	0.144
350	346.757	39.063	37.4	0.152
400	395.926	46.138	37.7	0.159
450	444.983	53.592	37.9	0.164
500	493.924	61.426	38.0	0.168
550	542.743	69.638	38.0	0.172
600	591.435	78.227	38.0	0.175

Continued.

ELEV = 30.0°

10	8.652	5.003	2.9	0.007
20	17.292	10.017	4.7	0.013
30	25.919	15.042	5.8	0.017
40	34.534	20.079	6.4	0.020
50	43.135	25.126	6.9	0.022
60	51.724	30.185	7.1	0.024
70	60.298	35.256	7.3	0.026
80	68.860	40.338	7.4	0.027
90	77.408	45.432	7.4	0.028
100	85.942	50.537	7.5	0.028
150	128.410	76.235	7.5	0.031
200	170.540	102.217	7.5	0.032
250	212.331	128.480	7.5	0.033
300	253.784	155.020	7.5	0.033
350	294.899	181.834	7.5	0.034
400	335.678	208.919	7.5	0.034
450	376.121	236.271	7.5	0.034
500	416.229	263.887	7.5	0.034
550	456.003	291.764	7.5	0.034
600	495.444	319.897	7.5	0.035

ELEV = 75.0°

10	2.584	9.677	2.4	0.002
20	5.161	19.317	3.3	0.003
30	7.780	28.978	3.7	0.004
40	10.292	38.641	3.8	0.004
50	12.846	48.305	3.9	0.004
60	15.393	57.969	3.9	0.005
70	17.932	67.635	3.9	0.005
80	20.468	77.302	3.9	0.005
90	22.936	86.965	3.9	0.005
100	25.503	96.628	3.9	0.005
150	37.971	144.997	3.9	0.005
200	50.256	193.381	3.9	0.005
250	62.362	241.788	3.9	0.005
300	74.230	290.219	4.0	0.005
350	86.027	338.673	4.0	0.005
400	97.636	387.170	4.0	0.005
450	109.078	435.649	4.0	0.005
500	120.321	484.169	4.0	0.005
550	131.435	532.710	4.0	0.005
600	142.373	581.272	4.0	0.005

---

Table 4.4: Consolidated table showing variations of  $N_0$ ,  $R$  and  $\epsilon$  for various climatic patterns.

1	2	3	4	5	6	7	8	9	10
Climatic type based on refractivity pattern	Charac-teristics of the areas of climatic types	Locations $N_0$ limits (Nunits)	Annual mean $N_0$ (Nunits)	Annual range of $N_0$ (Nunits)	Range of error for 300 Kms range & $\theta_0 = 0.5^\circ$	Mean of Range error (Meters) (Meters)	Elevat-ion error (Deg.)	Mean of elevation error (Deg.)	
CONTIN- ENTAL (Arid Zone[11])	Season- al ext- remes of temperatu- re & rainfall	Jodhpur New Delhi to Allahabad. Nagpur	305 to 390	330 to 350	70 to 80	69 to 90	76.9 to 79.5	0.199 to 0.165	0.230 to 0.246
SUBTRO- PICAL (Monsoon climate [11])	Regions with vegetation and rivers with de-finite rainy & dry seasons	Calcutta to Bombay	330 to 370	360 to 370	50 to 60	74 to 91	83 to 83.5	0.240 to 0.275	0.255 to 0.258
TROPICAL (hot and humid climate [11])	Tropical stations with low elevation & small seasonal variation of temperature	Madras to Trivan-drum	360 to 382	360 to 380	20 to 50	82 to 89	85.1 to 85.6	0.240 to 0.265	0.252 to 0.255

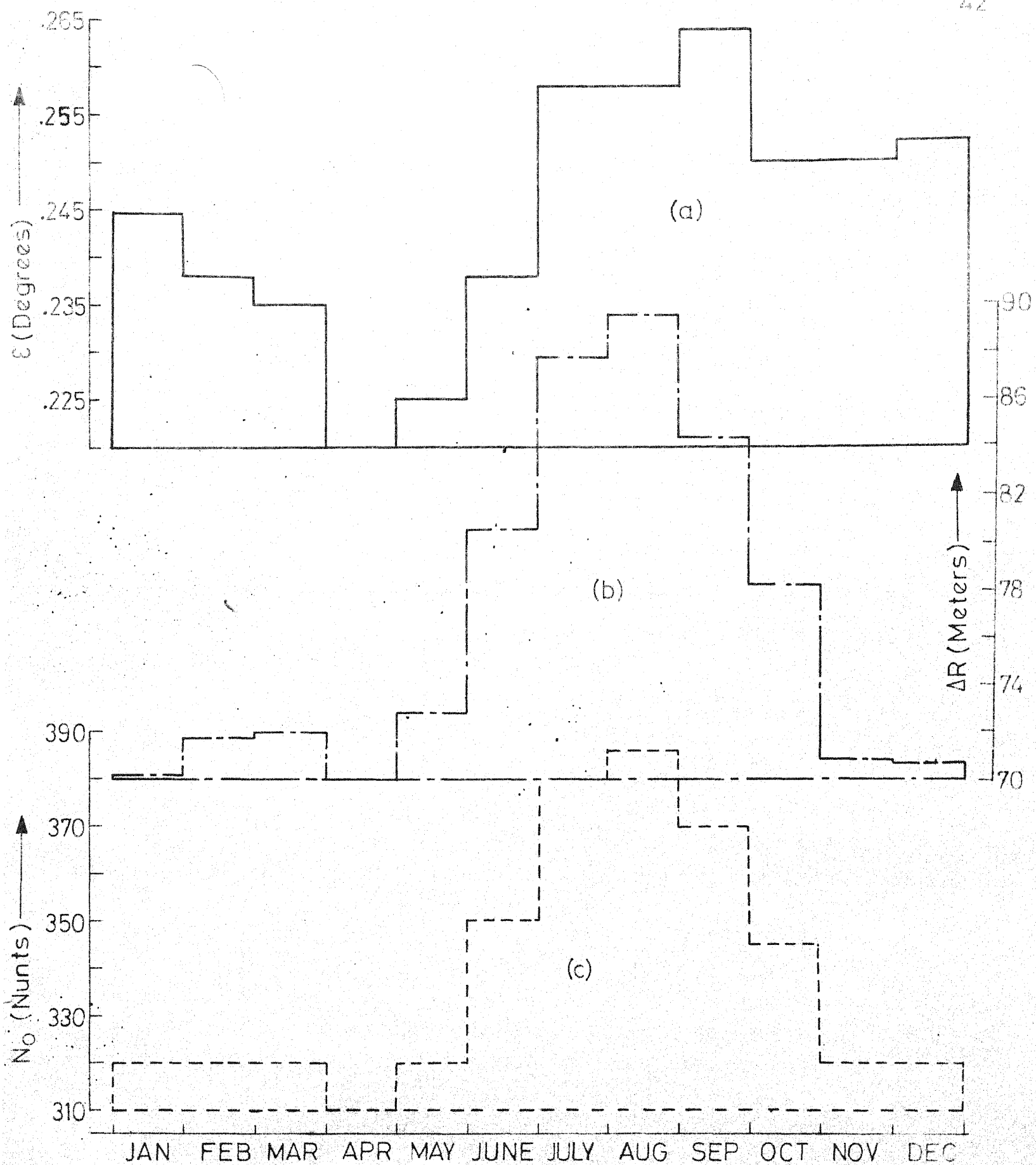


FIG. 4-2 HISTOGRAMS OF (a) MAXIMUM ELEVATION ANGLE ERROR  
(b) MAXIMUM RANGE ERROR, AT RADAR RANGE OF 300 kms.  
AND ELEVATION OF  $0.5^\circ$  AND (c)  $N_0$  FOR DELHI.

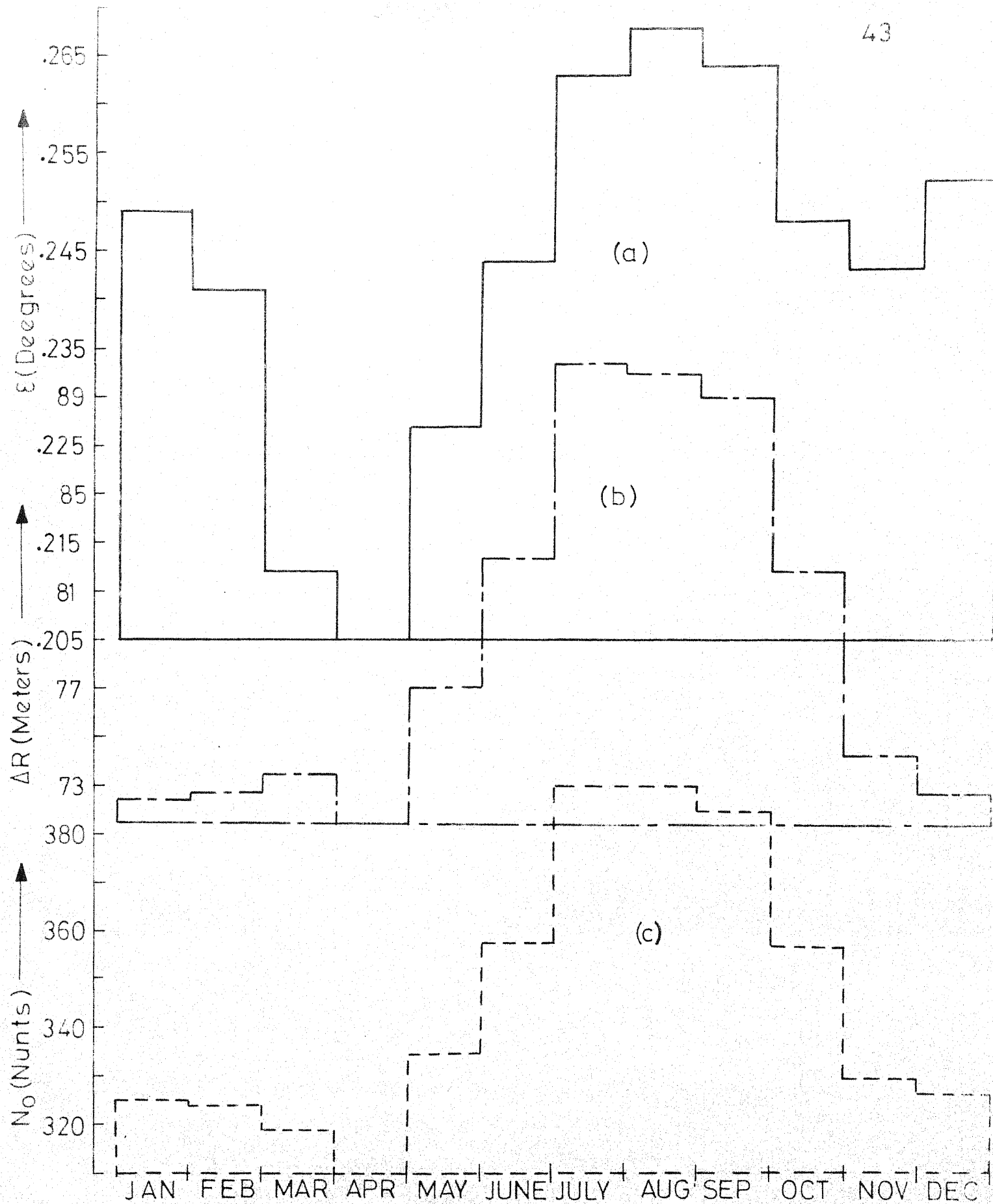


FIG. 4-3 HISTOGRAMS OF (a) MAXIMUM ELEVATION ANGLE ERROR  
(b) MAXIMUM RANGE ERROR, AT RADAR RANGE OF 300 km  
AND ELEVATION ANGLE OF 0.5° AND (c)  $N_0$  FOR ALLAHABAD



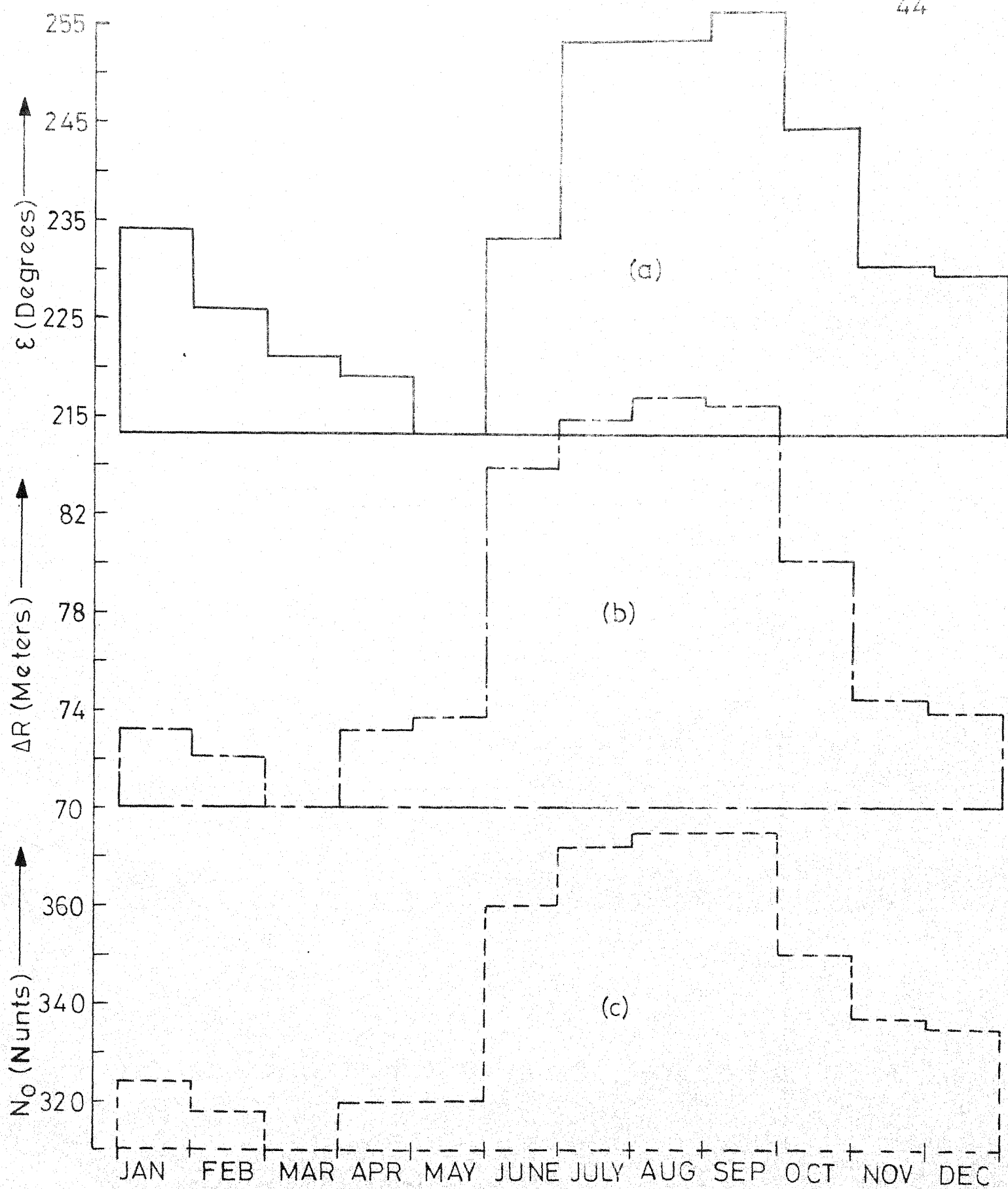


FIG. 4-4 HISTOGRAMS OF (a) MAXIMUM ELEVATION ANGLE ERROR (b) MAXIMUM RANGE ERROR, AT RADAR RANGE OF 300 kms. AND ELEVATION ANGLE OF  $0.5^\circ$  AND (c)  $N_0$  FOR NAGPUR.

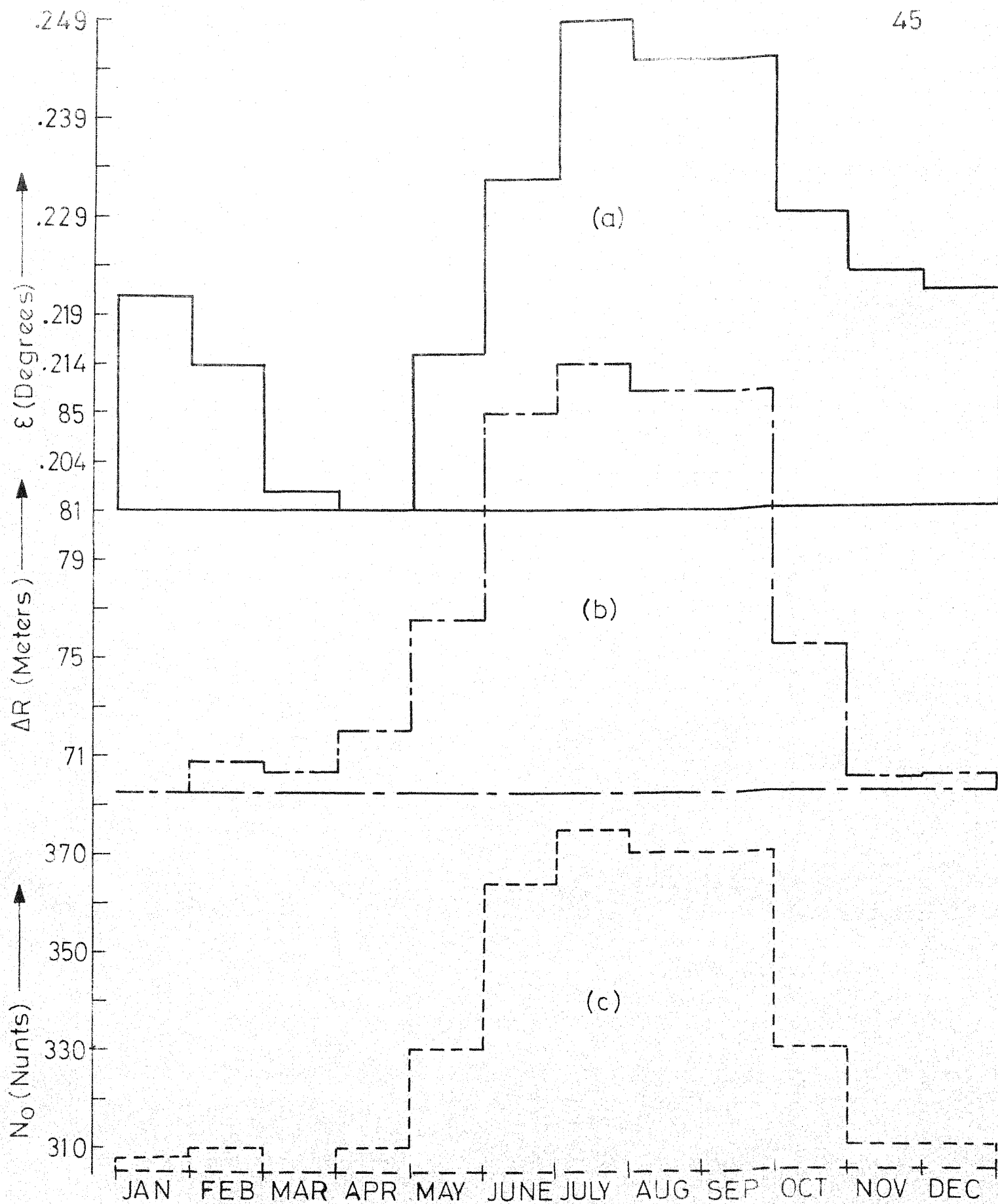


FIG. 4-5 HISTOGRAMS OF (a) MAXIMUM ELEVATION ANGLE ERROR  
(b) MAXIMUM RANGE ERROR, AT RADAR RANGE OF 300 kms.  
AND ELEVATION ANGLE OF  $0.5^\circ$  AND (c)  $N_0$  FOR JODHPUR.

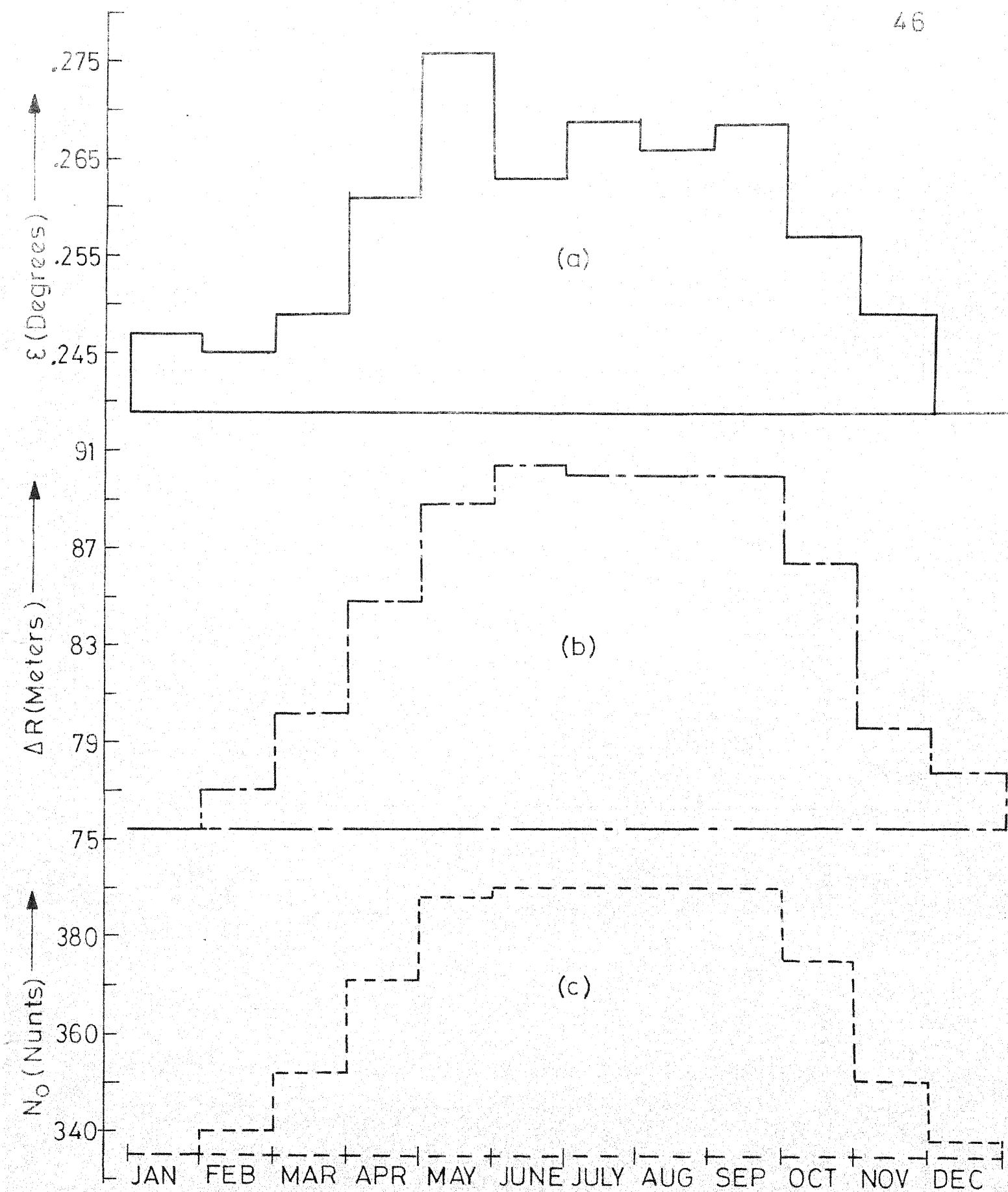


FIG.4-6 HISTOGRAMS OF (a) MAXIMUM ELEVATION ERROR (b) MAXIMUM RANGE ERROR, AT RADAR RANGE OF 300kms. AND ELEVATION ANGLE OF  $0.5^\circ$  AND (c)  $N_0$  FOR CALCUTTA.

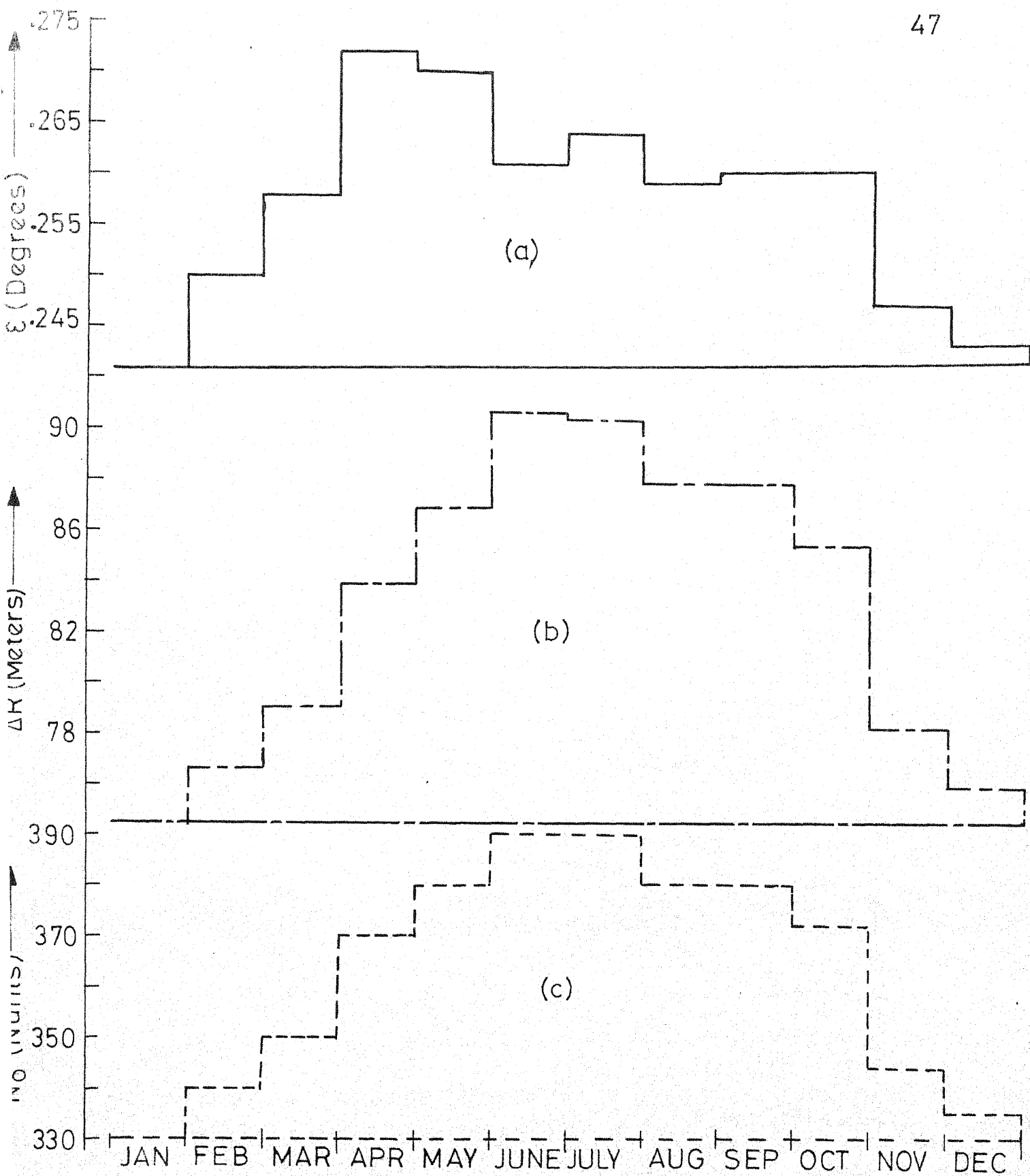


FIG. 4.7 HISTOGRAMS OF (a) MAXIMUM ELEVATION ERROR (b) MAXIMUM RANGE ERROR, AT RADAR RANGE OF 300 kms. AND ELEVATION ANGLE OF  $0.5^\circ$  AND (c)  $N_0$ . FOR BOMBAY.

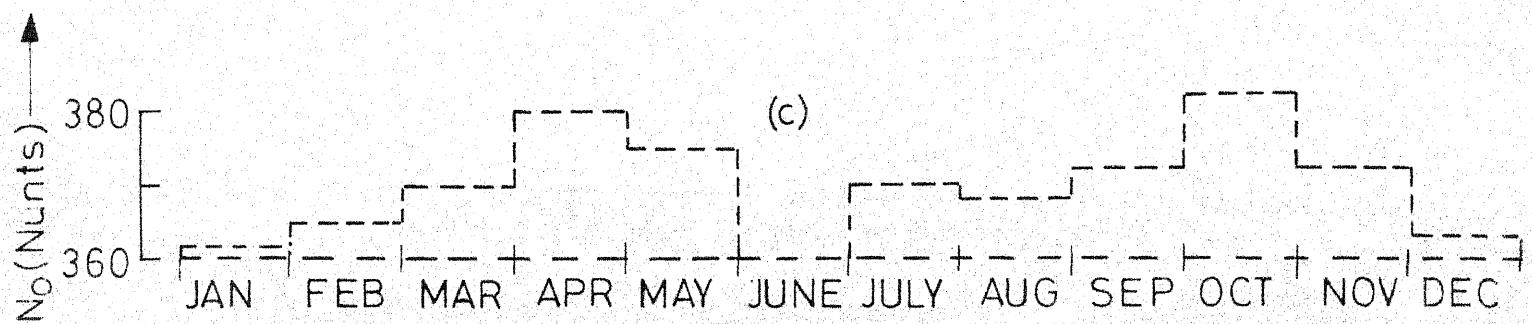
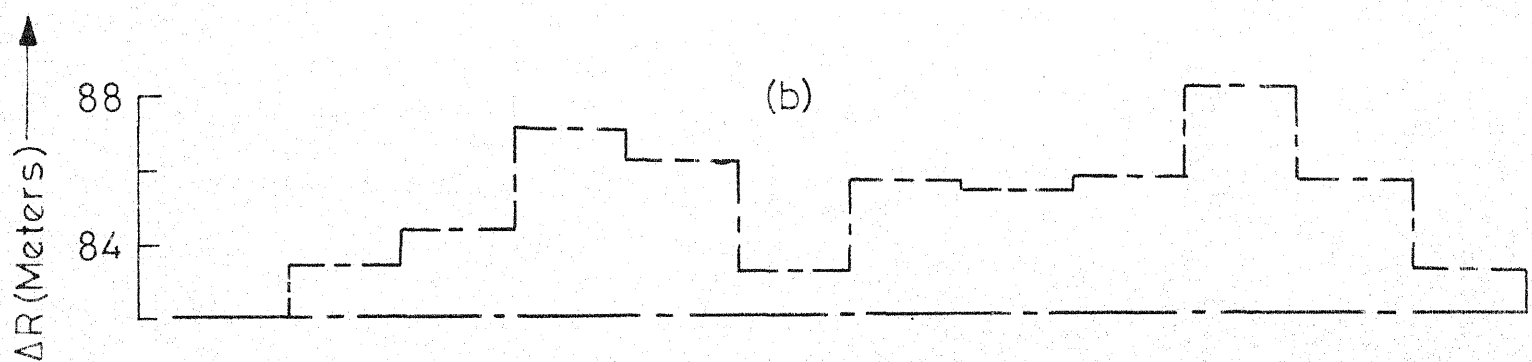
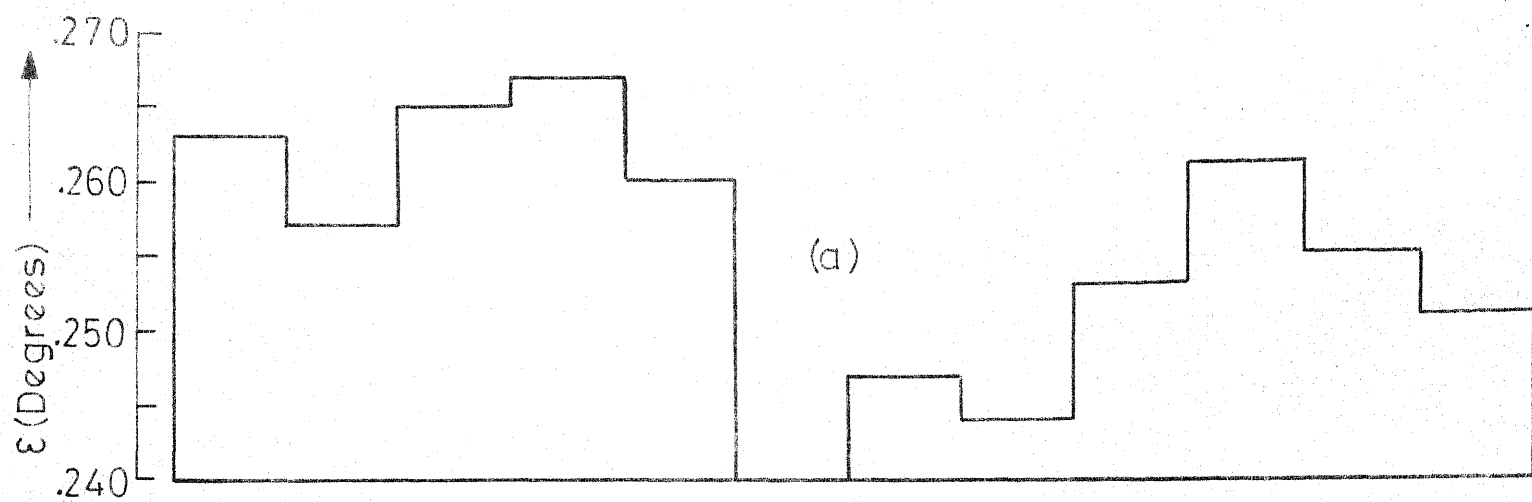


FIG. 4-8 HISTOGRAMS OF (a) MAXIMUM ELEVATION ERROR (b) MAXIMUM RANGE ERROR, AT RADAR RANGE OF 300 kms AND ELEVATION ANGLE OF  $0.5^\circ$  AND (c)  $N_0$  FOR MADRAS

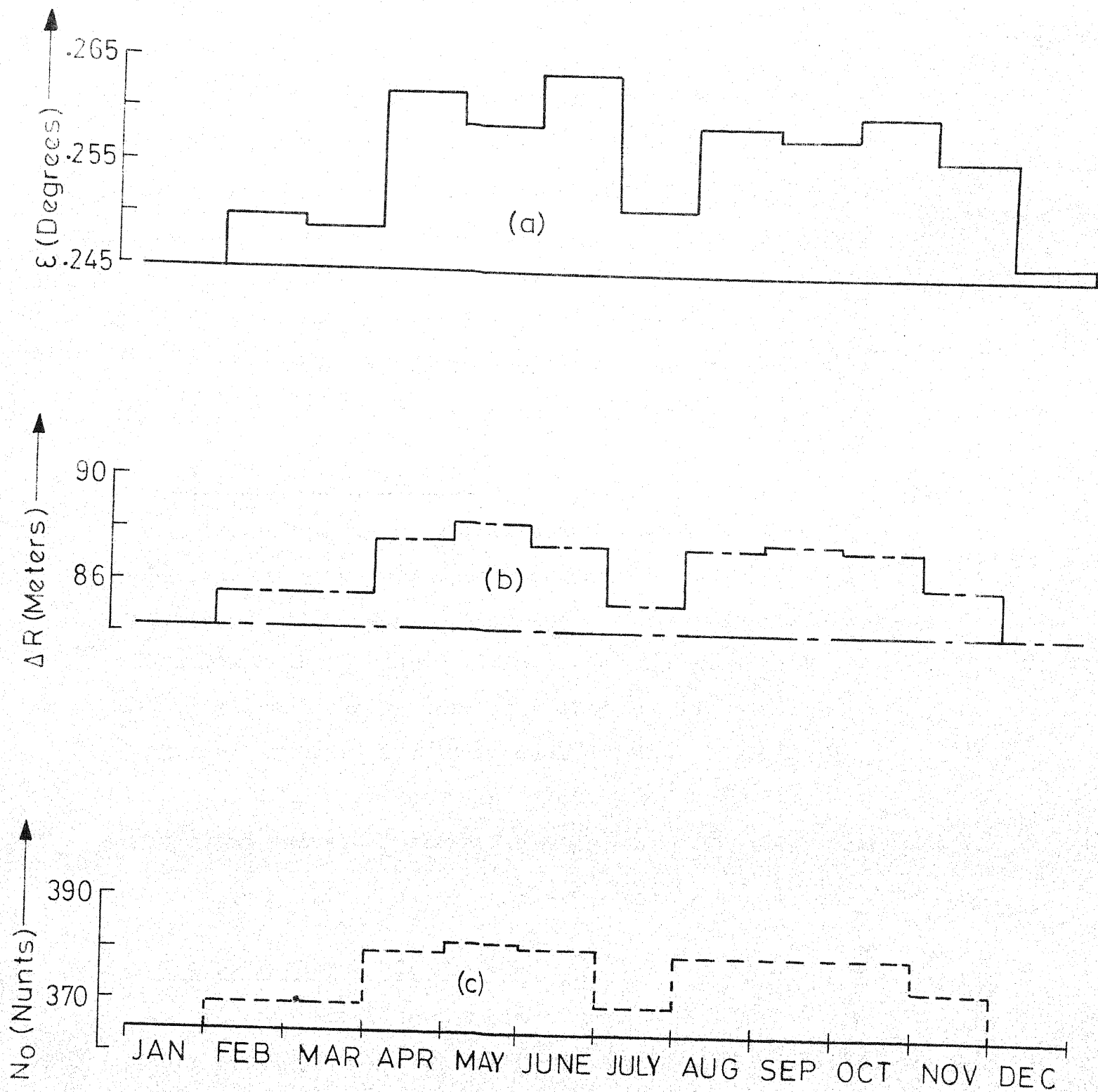


FIG. 4-9 HISTOGRAMS OF (a) MAXIMUM ELEVATION ERROR (b) MAXIMUM RANGE ERROR, AT RADAR RANGE OF 300 kms. AND ELEVATION ANGLE OF  $0.5^\circ$  AND (c)  $N_0$  FOR TRIVANDRUM.

was also observed that general shape of the histograms remains the same for all other values of radar range.

A computer program was developed to plot the errors versus radar range curves on IBM 1800. Maximum and minimum errors along with the errors based on yearly average of  $N_0$  were drawn for all the eight places for ranges varying from 10 Km to 600 Km and for elevation angles of  $0.5^\circ$ ,  $15^\circ$  and  $75^\circ$ . These curves were smoothened wherever required, particularly at low error values of elevation angle error curves so as to avoid the inherent incapability of IBM 1800. These curves are given from Figures 4.10 to 4.17.

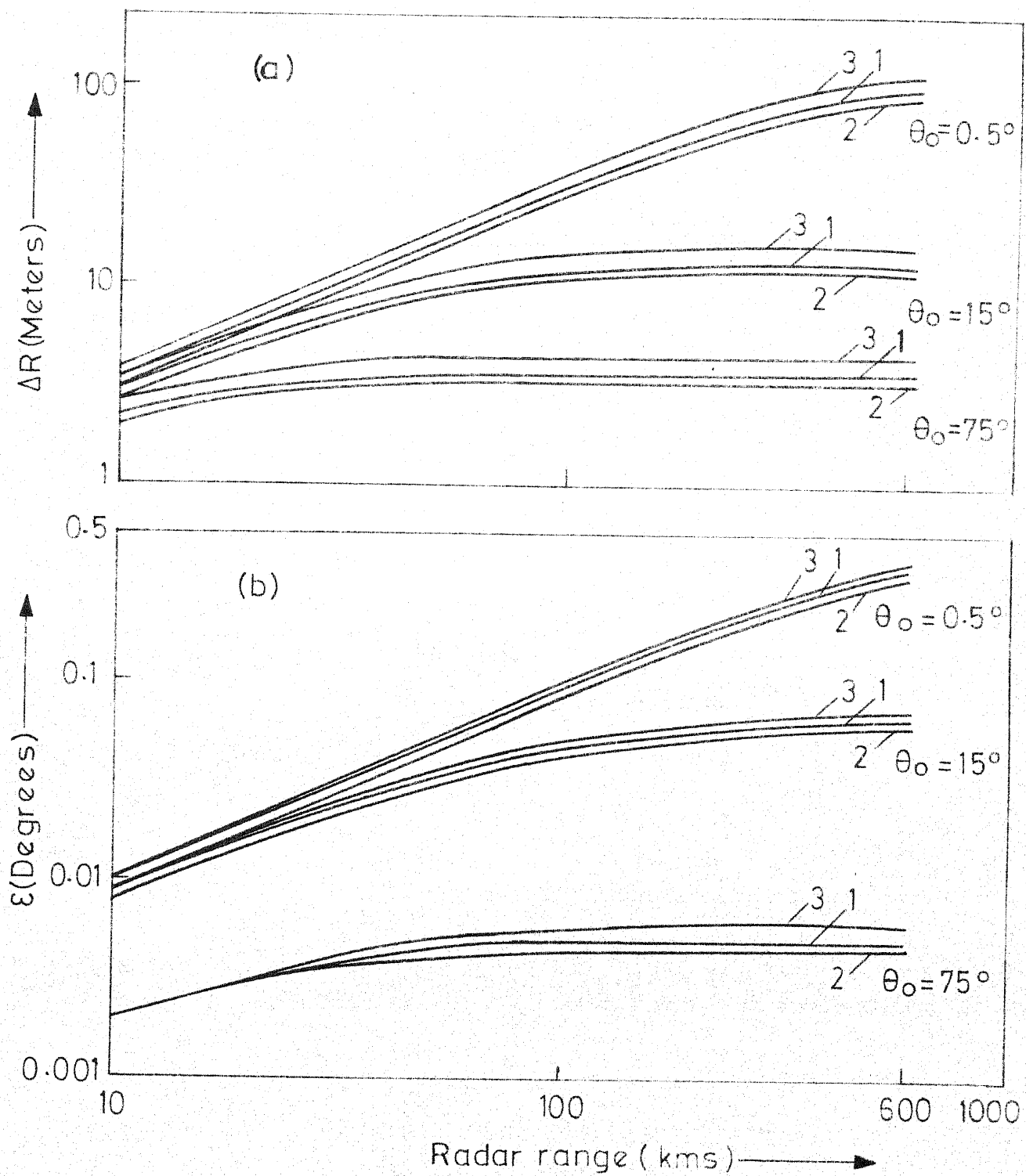
#### 4.4 Radar Coverage Diagrams

Range-height-angle charts are important for many radar applications. Radar coverage diagrams are plots of radar range versus elevation angle, and form a part of such general plots. A version of these charts is drawn in Figure 4.18(a) for New Delhi based on yearly mean value of  $N_0$ . Slight variation in this diagram is expected for individual months, this being due to variation of  $N_0$  over the year. Height versus ground range curves for various values of elevation angle are drawn in Figure 4.18(b).

Curves for Madras and Calcutta can be similarly drawn.

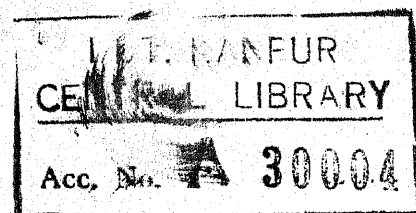
#### 4.5 Height versus Error Curves

If the target height and elevation angle  $\theta_0$  are known, then a quick procedure for correcting the errors can be formulated by drawing height versus error curves for various elevation angles. These curves are given in Figure 4.19 for Delhi for maximum elevation and range errors. Normal aircraft ceiling heights are taken in these curves. Similar curves can be drawn for Madras and Calcutta.

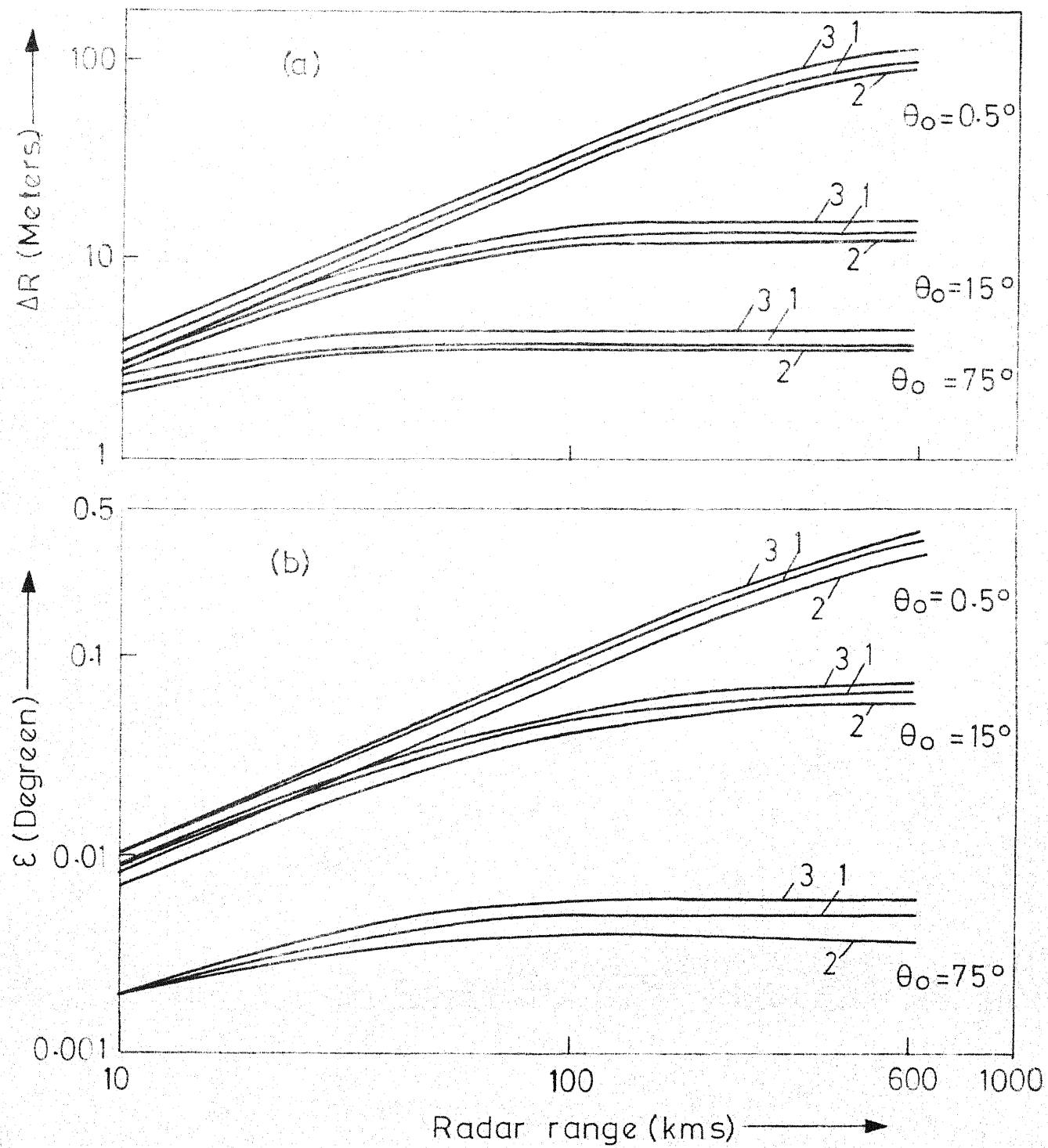


Legend 1. Yearly mean 2. Minimum error. 3. Maximum error.

FIG. 4-10 (a) RANGE ERROR (b) ELEVATION ANGLE ERROR CURVES FOR DELHI.

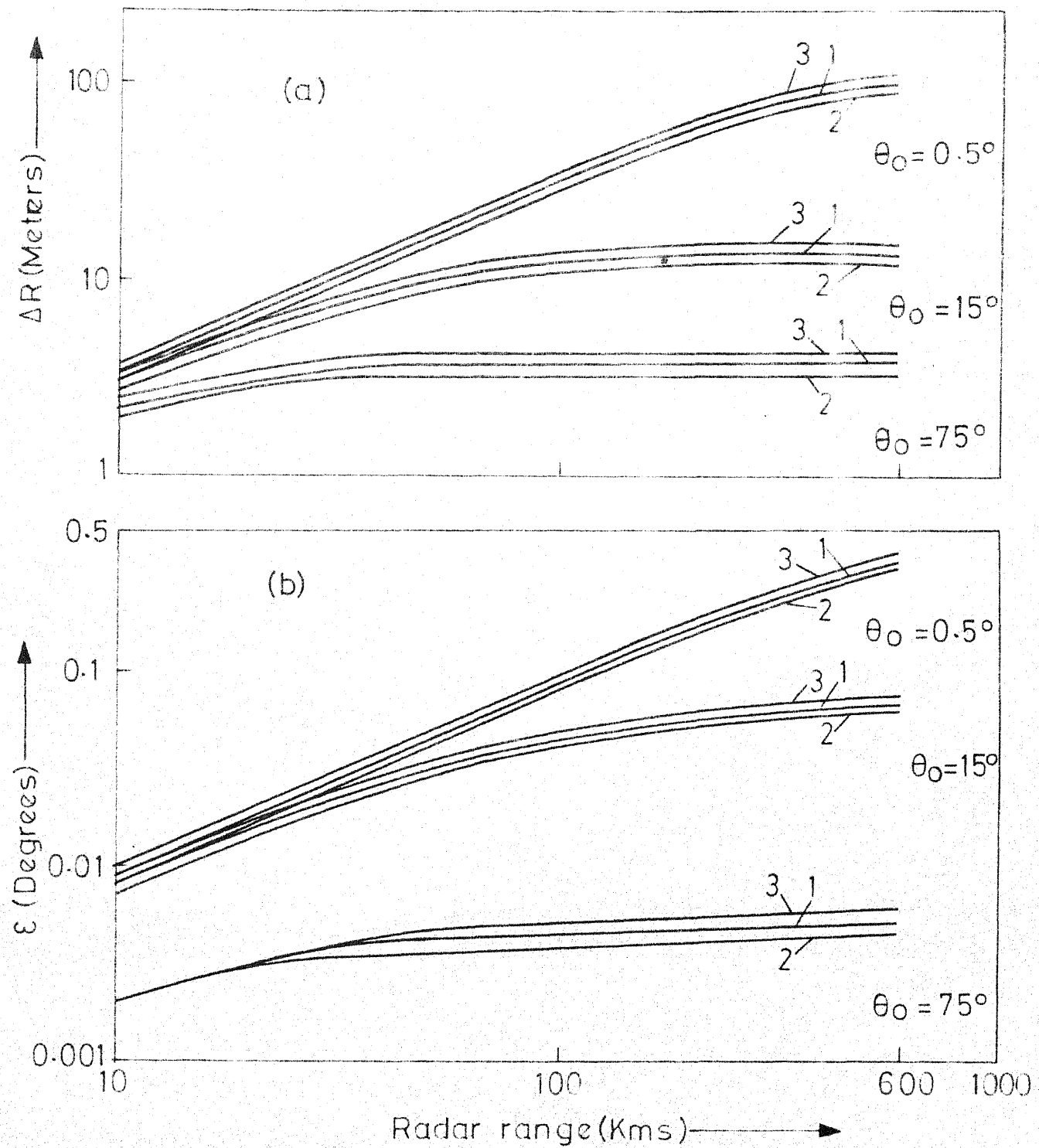






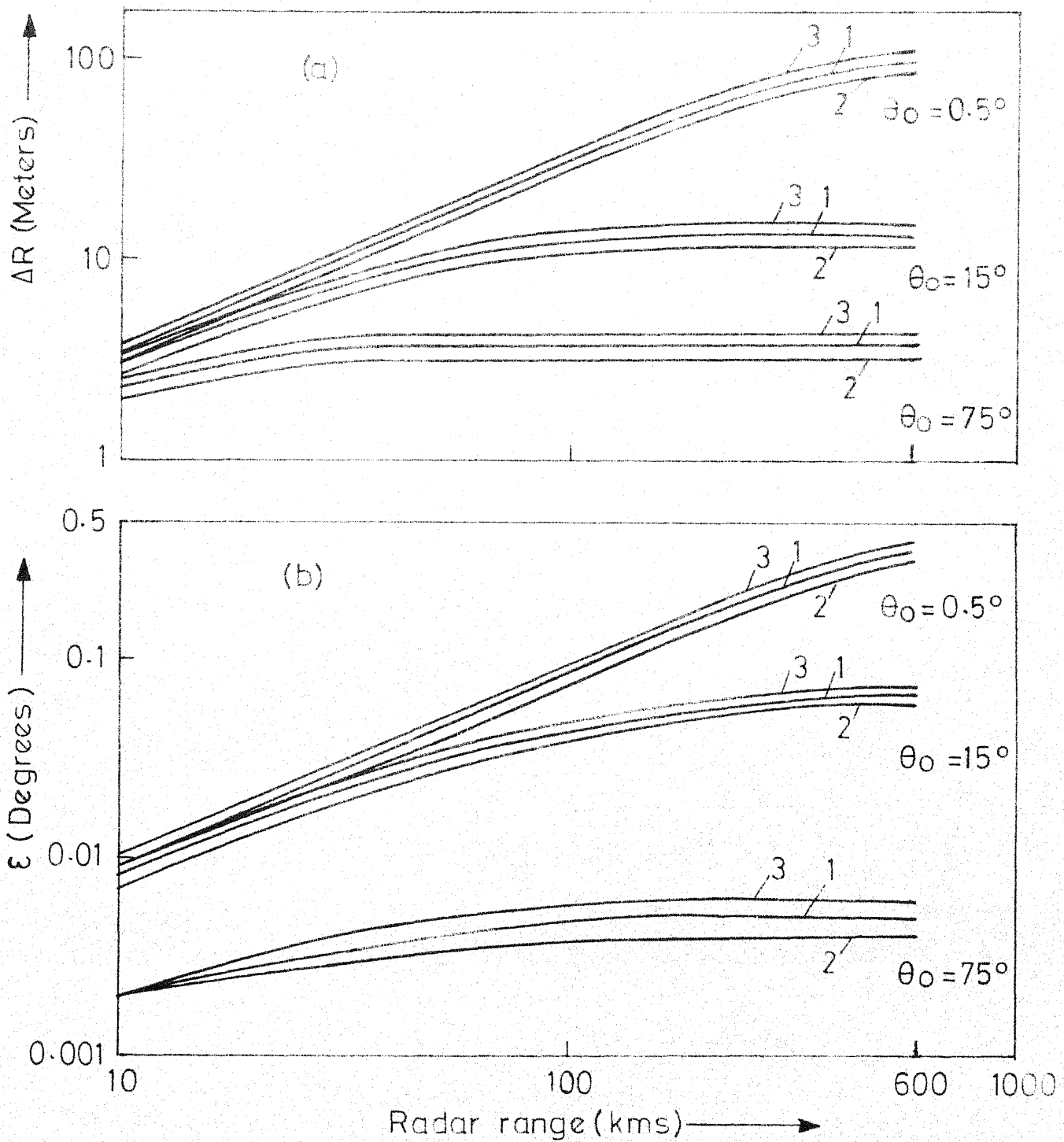
Legend:-1. Yearly mean. 2. Minimum error 3. Maximum error.

FIG.4-11 (a) RANGE ERROR (b) ELEVATION ANGLE ERROR CURVES FOR ALLAHABAD.



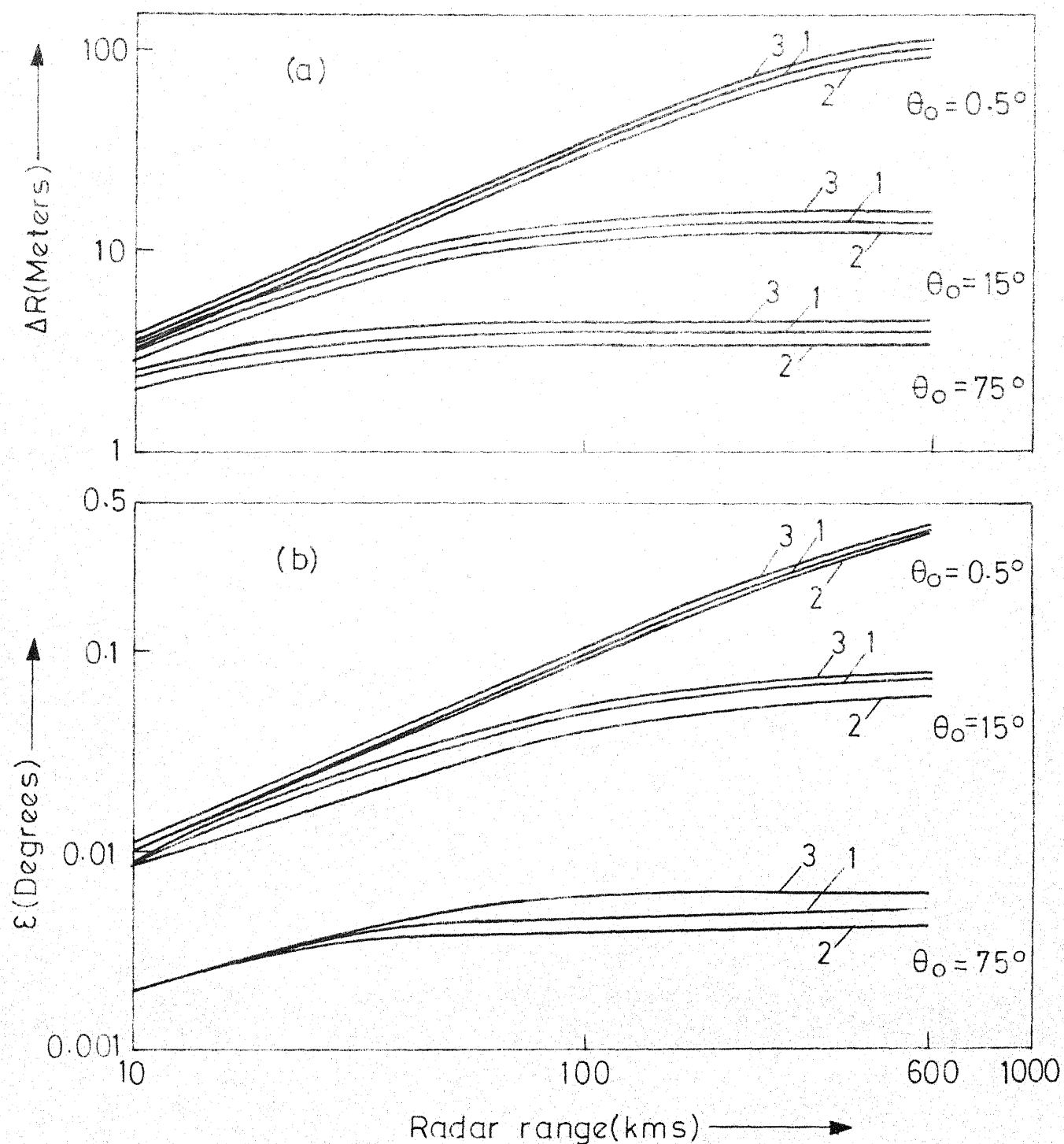
Legend:- 1. Yearly mean. 2. Minimum error. 3. Maximum error.

FIG. 4-12 (a) RANGE ERROR (b) ELEVATION ANGLE ERROR CURVES FOR NAGPUR.



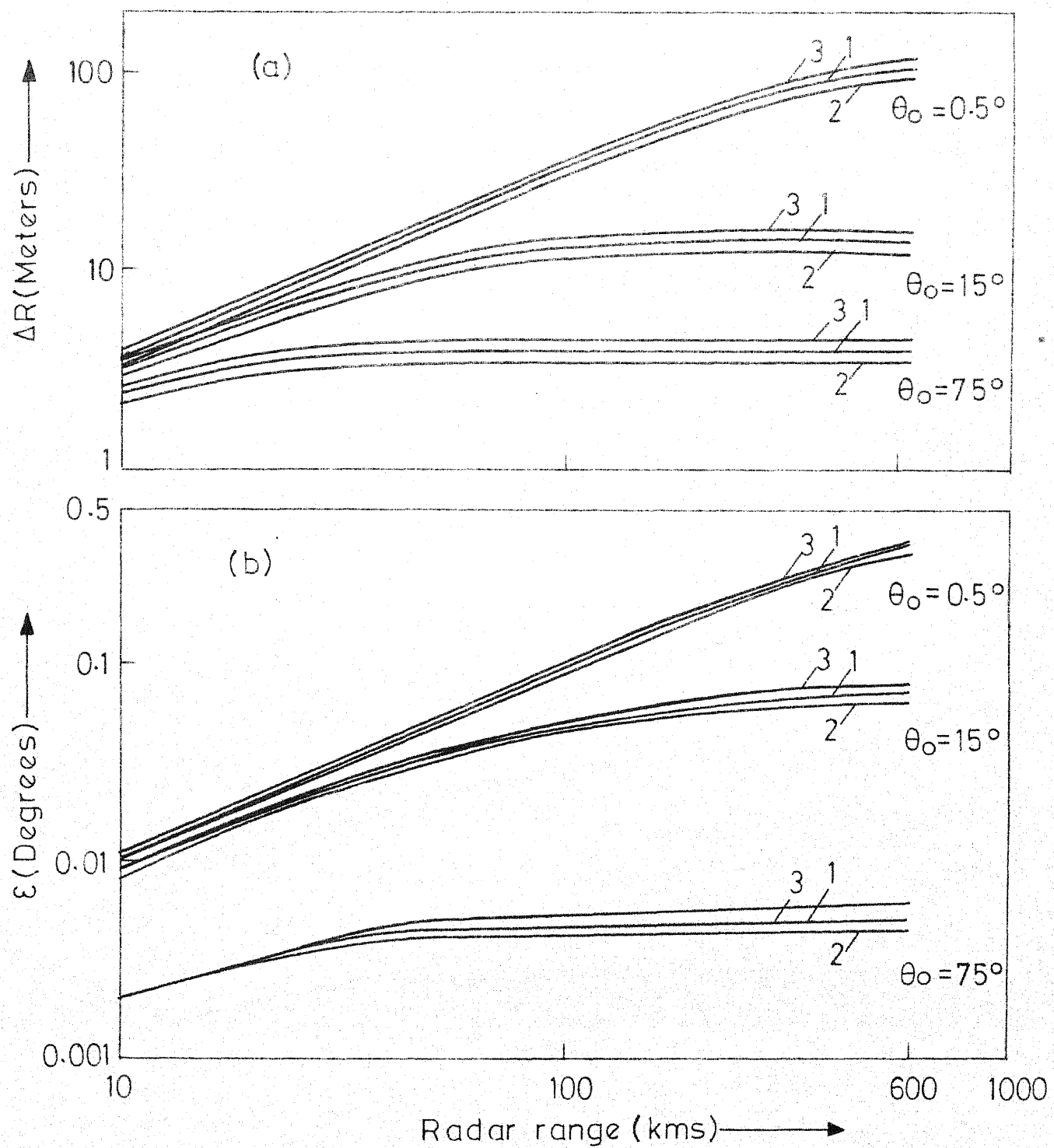
Legend:- 1. Yearly mean 2. Minimum error 3. Maximum error.

FIG.4-13 (a) RANGE ERROR (b) ELEVATION ANGLE ERROR CURVES FOR JODHPUR.



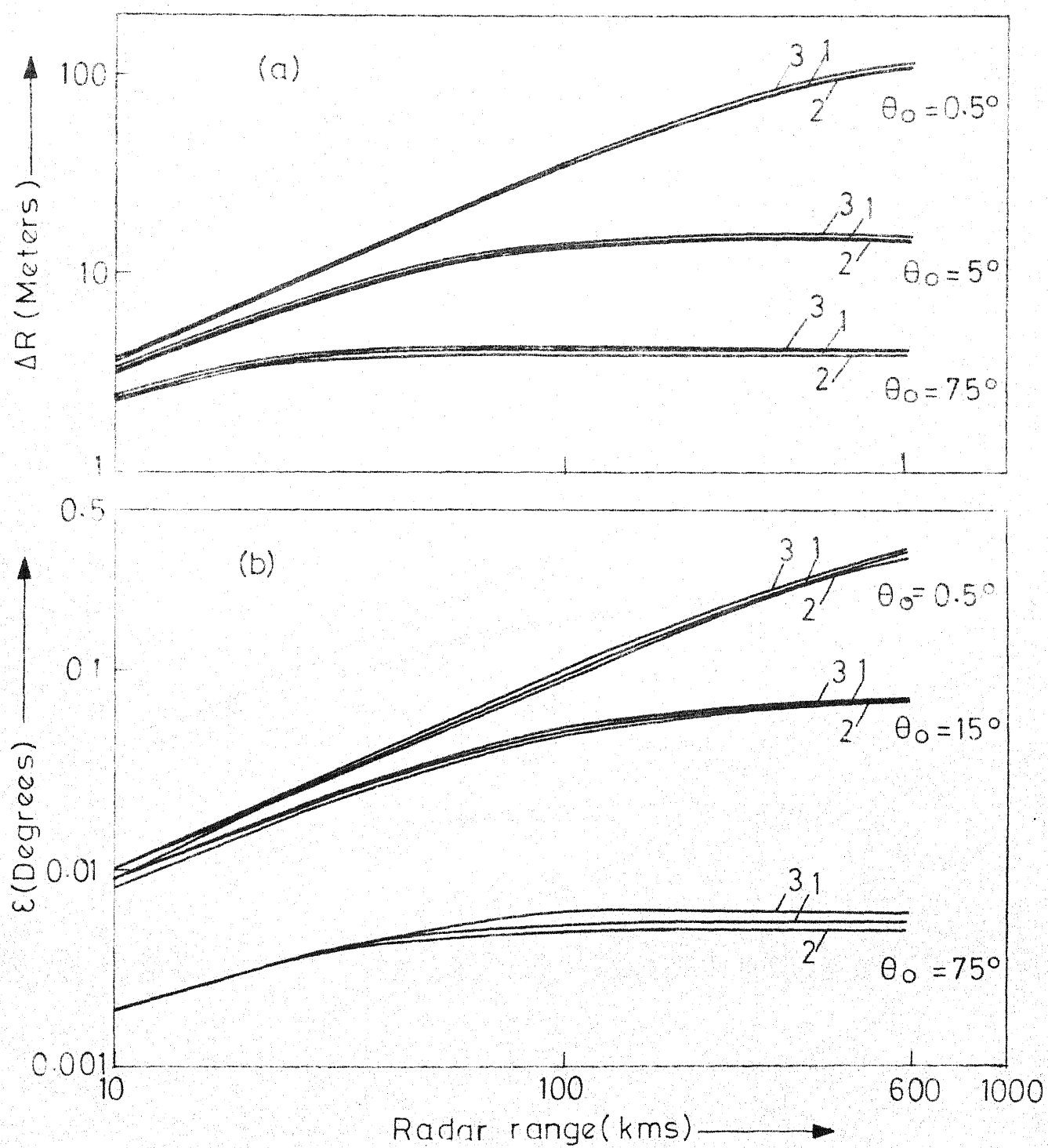
Legend:- (a) Yearly mean 2. Minimum error 3. Maximum error.

FIG. 4-14 (a) RANGE ERROR (b) ELEVATION ANGLE ERROR CURVES FOR CALCUTTA.



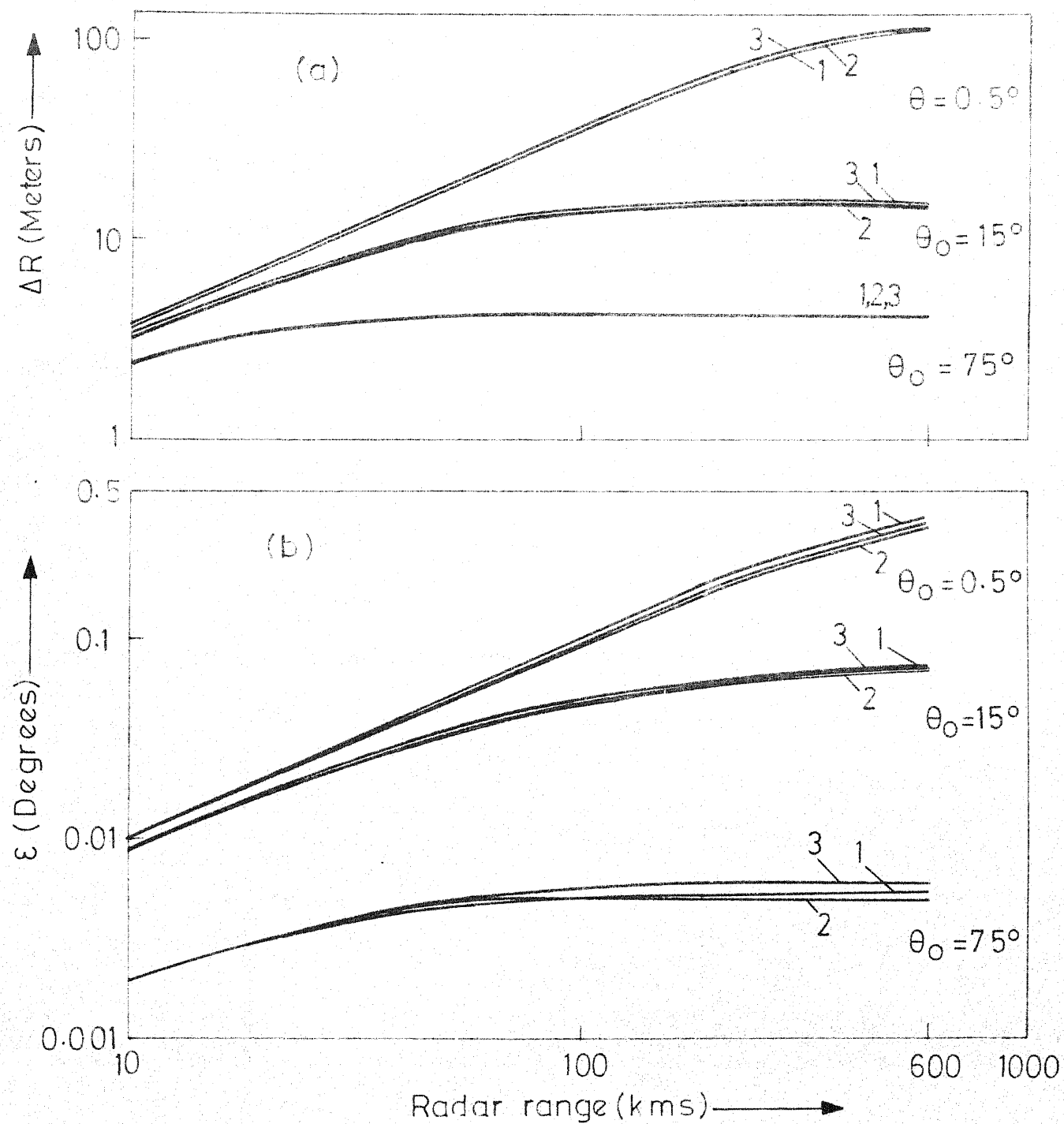
Legend:-1. Yearly mean 2. Minimum error 3. Maximum error.

FIG. 4-15 (a) RANGE ERROR (b) ELEVATION ANGLE ERROR CURVES FOR BOMBAY.



Legnd:- 1. Yearly mean 2. Minimum error. 3. Maximum error.

FIG. 4.16 (a) RANGE ERROR (b) ELEVATION ANGLE ERROR CURVES FOR MADRAS.



Legend:- 1. Yearly mean 2. Minimum error 3. Maximum error.

FIG.4-17. (a) RANGE ERROR (b) ELEVATION ANGLE ERROR CURVES FOR TRIVANDRUM.

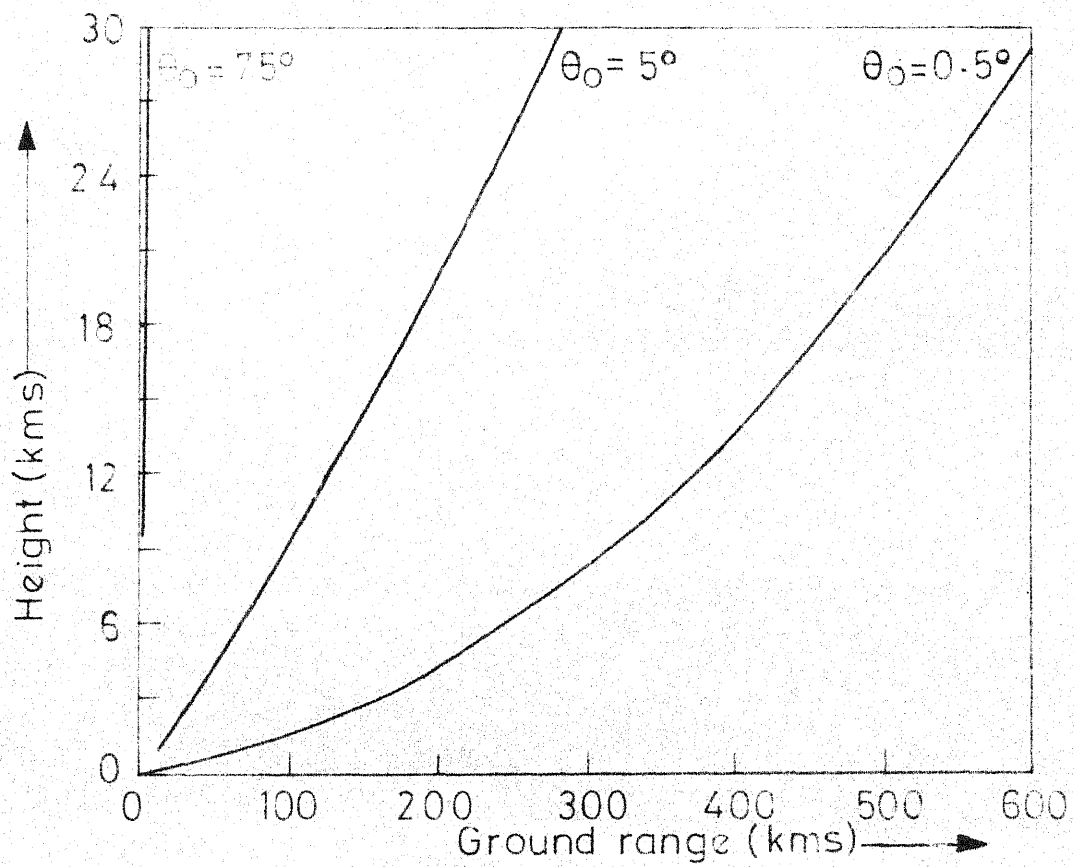
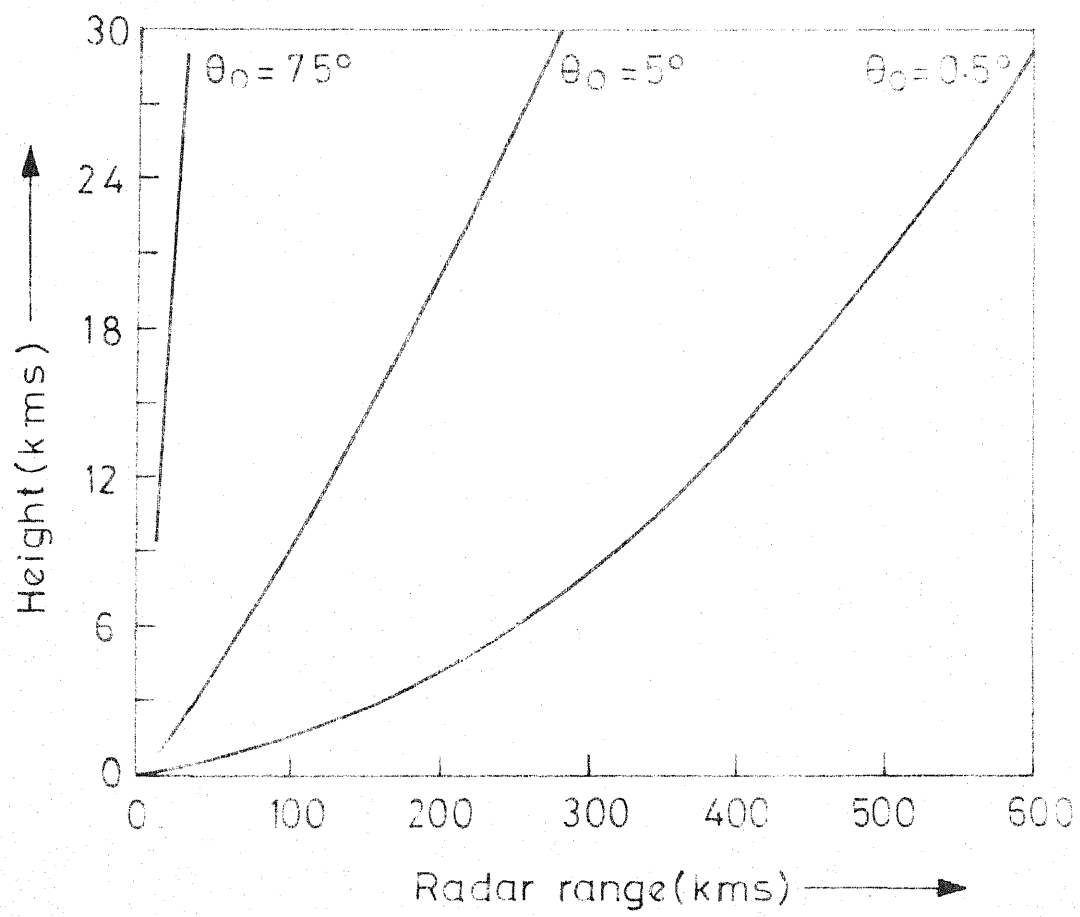


FIG 4-13 RADAR COVERAGE DIAGRAMS FOR YEARLY MEAN VALUES OF  $N_0$  FOR DELHI.



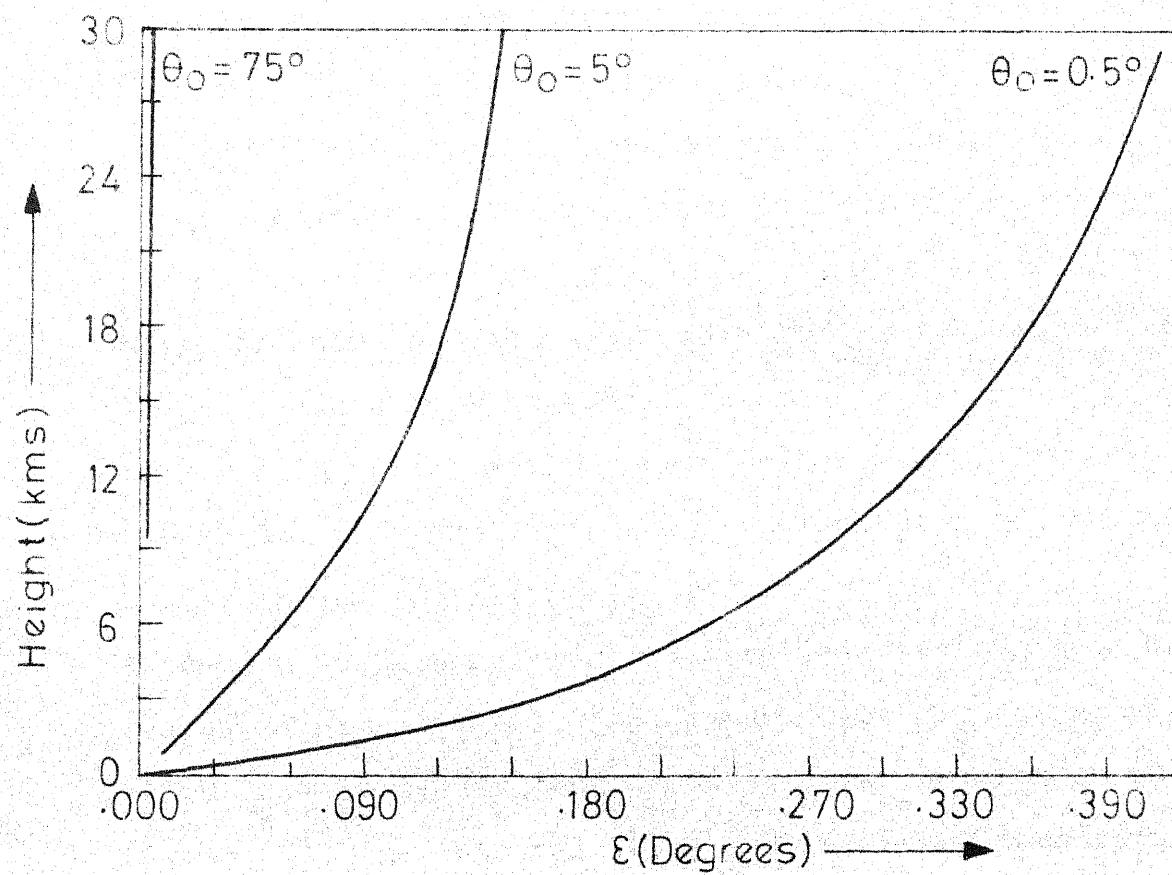
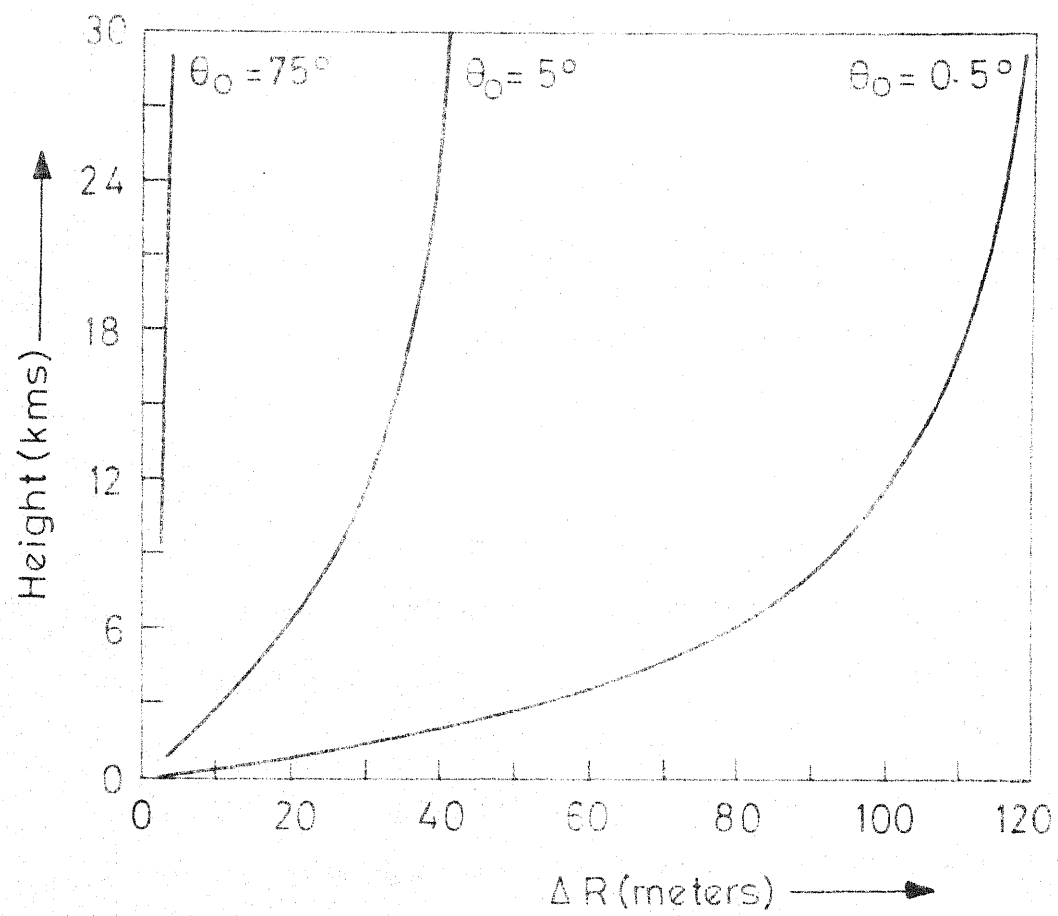


FIG. 4-19 (a) HEIGHT Vs. MAXIMUM RANGE ERROR &  
(b) HEIGHT Vs. MAXIMUM ELEVATION ANGLE ERROR  
CURVES FOR DELHI.

## CHAPTER V

NUMERICAL SIMULATION OF TROPOSPHERE OVER DELHIBY MONTE-CARLO TECHNIQUES5.1 Introduction

In the last chapter, the monthly average  $N_0$  values have been used for finding various parameters for the target. Actually there is a marked variation in the  $N_0$  values with time and enough of  $N_0$  data is not available for analysing the problem exhaustively. Accordingly a large number of values of  $N_S$ , the surface refractivity, have been generated for simulation of troposphere over Delhi, and this is based on the law of large numbers and the central limit theorem which states that the combined distribution for a large number of random variables tends to a normal distribution and the variance is small for large numbers. To start with, the distribution is assumed to be normal and the mean ( $= 332N$  units) and the standard deviation ( $= 25 N$  units) of known  $N_S$  values are used for random generation of 1000  $N_S$  values by Monte-Carlo techniques for the simulation of the tropospheric conditions over Delhi. The term Monte-Carlo is frequently reserved for the use of stochastic techniques for solving an essentially deterministic problem and due to this the random numbers generated are called pseudo random numbers. Program of appendix 'B' [25] is used for generating these pseudo random  $N_S$  values. First uniformly distributed random numbers are generated in the interval (0,1) and these are then converted to numbers in normal distribution.

## 5.2 Set up for Simulation of Troposphere

Once  $N_S$  values are generated, the decaying constant  $C_e$  per Km can be found out for each of these, from the relation

$$C_e = \ln\left(\frac{N_S}{N_S - \Delta N}\right) \quad (5.1)$$

where  $\Delta N$  is the average of the monthly values for CCIR recommended months of February, May, August and November for 00 GMT and 12 GMT [26].

The computer program of Appendix 'A' was modified to take these changes into account and elevation angle and range errors were found for different values of  $N_S$  for a target having a range of 300 Kms and an elevation angle of  $0.5^\circ$ . This program was also used to find the means and standard deviations of  $N_S$ , elevation angle and range errors.

## 5.3 Results

Density distribution curves for the resulting error values are drawn in Figure 5.1, and on calculation it was found that, as expected,  $N_S$  values follow a normal distribution. Means and standard deviations of  $N_S$ ,  $\Delta R$  and  $\epsilon$  for these 1000 generated values of  $N_S$  are

Mean value of	$N_S = 337 \text{ N units}$
	$\Delta R = 67.9 \text{ meters}$
	$\epsilon = 0.268^\circ$

Standard deviation of	$N_S = 27$ N units
	$\Delta R = 1.3$ meters
	$\epsilon = 0.063$ degrees

Mean and standard deviation of  $N_S$  are comparable to the known yearly average values for Delhi. Mean value of  $\epsilon$  is slightly higher than and that of  $\Delta R$  is slightly lower than the known yearly average values for Delhi and a significant contribution to this difference is due to the approximations used in the determination of  $\Delta N$ . The standard deviations of errors from their means are comparable to the reported values for various places in the world.

## CHAPTER VI

DISCUSSION OF RESULTS AND CONCLUSION

Radar range and elevation angle errors which arise due to the refractivity variations of the troposphere are discussed in this thesis. These errors are of great importance for long range surveillance radar systems. Errors have been calculated for eight radio sonde stations for all the twelve months and their yearly average for known monthly average  $N_0$  values, for a target varying in ranges from 10 Kms to 600 Kms and in elevation angle from  $0.5^\circ$  to  $75^\circ$ . The various results of the calculations are given in Chapter IV. It is observed that in all cases the elevation angle and range errors of the target are having a maximum value for lowest value of target elevation angle of  $0.5^\circ$  for all ranges. These errors carry on decreasing with increasing elevation angles of the target for any typical target range. Also, for a fixed elevation angle of the target, the errors increase with increase in range. Various histograms of Chapter IV indicate the average monthly variation of the maximum errors for typical target range of 300 Kms and elevation angle of  $0.5^\circ$  for all the eight places. General pattern for individual places was found out to be the same for different values of range and elevation angle of the target. A version of radar coverage diagram is given in Chapter IV; which can be used to find any one of the three parameters provided the other two are given out of  $h, R, \theta_0$  or  $h, G, \theta_0$ . Also a method of

error correction is given which can be used for quick determination of the true target fix in case the target elevation angle and the height is known.

Monte-Carlo techniques were used for numerical simulation of troposphere over Delhi by generating 1000 normally distributed pseudorandom ( $N_S$ ) numbers by assuming a normal distribution for known monthly average  $N_S$  values over Delhi. The results are given in Chapter V and the calculated means and standard deviations of  $N_S$ ,  $\Delta R$  and  $\epsilon$  are found to be comparable to published data and the known values for Delhi.

In this thesis, elevation angle and range errors of a target have been analysed for eight stations in India. This can be extended to cover up more regions of Indian peninsula. Other effects, like, doppler effect and attenuation of the signal, which also are caused by the refractivity variation of the troposphere can be calculated for various places for various values of range and elevation angle of the target.

A COMPUTER PROGRAM FOR THE DETERMINATION OF HEIGHT,  
GROUND RANGE, TRUE RANGE, TRUE ELEVATION ANGLE,  
ELEVATION ANGLE ERROR AND RANGE ERROR OF A TARGET  
OF VARYING RANGES AND APPARENT ELEVATION ANGLES.

SIBFTC MAIN

```

C   TROPOSPHERIC PROPAGATION ERRORS IN RADAR MEASUREMENT IN INDIA
C   *****
C   CALCULATION OF ELEVATION AND RANGE ERRORS VERSUS RANGE FOR
C   VARIOUS ELEVATION ANGLES OF RAY PATH
C   THE RAY HEIGHT IS COMPUTED AT SPECIFIED RANGE AND ELEVATION
C   ANGLE
C   FOR STANDARD NEGATIVE EXPONENTIAL REFRACTIVITY ATMOSPHERE
C   THE RANGE AND HEIGHT ARE GIVEN IN KMS AND ELEVATION ANGLE IN
C   DEGREES
C   REF = NS * ( 10 ** -6), GRAD = CE PER METER
C   NS AND CE VALUES ARE TAKEN FROM RTRC MONOGRAM NO.1 BY
C   VENKITESHWARAN ETAL (FEB 1970)
C   CE DENOTES THE REFRACTIVITY GRADIENT PER METER
C   NS IS THE REFRACTIVITY AT THE SURFACE IN N UNITS
C   N0 IS THE VALUE OF NS CONVERTED TO SEA LEVEL IN N UNITS
C   ELEVATION IS THE INITIAL ELEVATION ANGLE OF RAY,  $\theta_0$ , IN DEGREES
C   RNG1 IS THE TERMINAL RANGE OF RAY, R, IN KMS
C   RNG DENOTES INTEGRATED RANGE, R, IN KMS
C   X1 DENOTES RAY HEIGHT, h, IN METERS
C   HMILES DENOTES RAY HEIGHT, h, IN KMS
C   GRG DENOTES GROUND RANGE, G, IN KMS
C   RNGERR DENOTES THE DIFFERENCE OF RAY PATH AND STRAIGHT LINE
C   DISTANCE OF THE TARGET,  $\Delta R$ , IN METERS
C   ELEVER DENOTES THE DIFFERENCE OF APPARANT ELEVATION ANGLE AND
C   TRUE ANGLE OF THE TARGET,  $\epsilon$ , IN DEGREES
C   NO1A AND NO1B DENOTE THE OUTPUT PARAMETERS OF THE SIMPSON'S
C   RULE NUMERICAL INTEGRATION SUBROUTINE, SIMCON
C   RADAR ANTENNA HEIGHT IS IGNORED IN THESE CALCULATIONS
C   TARGET HEIGHT IS TAKEN WRT SEA LEVEL
C   GROUND RANGE IS DISTANCE ALONG THE ASSUMED SPHERICAL EARTH AT
C   SEA LEVEL
C   *****
COMMON /B/ REF, RAD, GRAD, CONST, U, A
EXTERNAL F1, F2
H3(R1, R2, SF) = SQRT(R1*R1+R2*R2+2.*R1*R2*SF) - R1
THT ( P1, RH, GR, HT, RD ) = ARCCOS( P1 / (( 1.+RH * (EXP ( -GR *
1HT ))) * (1. + HT / RD )))
ARG(A1, B1, C1, X) = (2.*A1*X-2.*SQRT(A1*C1) + 2.* SQRT(A1* (A1*
1X*X+ B1 * X + C1)))/(B1+ 2.0* SQRT( A1* C1))
DATA RAD / 6.373E+06 /
PRINT 600
X0 = 100.0
XA = 5000.0

```

```

XB = 70000.0
CONST = 0.001
PIE = 3.14159265
APPA = 180.0/PIE
PAPA = 1.0/APPA
H = 1.0
NSIG = 6
MAXN = 10
PREC = 10.0 ** ( - NSIG )
1 READ 500, REF, GRAD, MONTH1, MONTH2
  IF ( REF .LT. 0.0 ) GO TO 499
500 FORMAT (F9.6, F10.7, 5X, 2A5 )
  PRINT 17, MONTH1, MONTH2, REF, GRAD
17 FORMAT ( 1 H0, 30X, 2A5//30X, * REF = *, F9.6 // 30X,*GRAD=*,
1F10.7 )
  AB = 1.0+REF
  RI = 1.0/RAD
  RS = RI*RI
  GAM = REF*GRAD/AB
  GS = GAM*GAM
  T = RAD*GAM
  FAC=1.0/(1.0-T)
  RAD1=RAD*FAC
  ELEV = 0.5
5 RNG1 = 10.0
  PRINT 993, ELEV
  RDN = ELEV * PAPA
  NN = 0
  DD 101 K = 1,20
  NN = NN + 1
  CT = COS ( RDN )
  SN = SIN ( RDN )
  S = SN * SN
  U = AB * AB * S - 2.0 * REF - REF * REF
  A = AB * CT
  RNG3 = RNG1 / CONST
  HMIN = H3 ( RAD1, RNG3, SN )
  HMAX = (H3 ( RAD, RNG3, SN )) * AB
  IF ( ELEV - 1.0 ) 56, 56, 57
56 Q = 2.0 * ((1.0 + S) * RI - GAM )
  QQ = 2.0 * (( 2.0 * GAM - RI ) * S - GAM + RI )
  P = GRAD * GAM + GS - 8.0 * GAM * RI + ( 5. + S ) * RS
  PP = GRAD * GAM - 7. * GS + 8. * GAM * RI - 3. * RS + S * ( 10.
1 * GS - 8. * GAM * RI - 2.0 * GRAD * GAM + 3.0 * RS )
  ARG1 = ARG( PP, QQ, S, H )
  ARG2 = ARG ( P, Q, S, H )
  CALL LOG1PL ( ARG1, 12, SUM1 )
  CALL LOG1PL ( ARG2, 12, SUM1 )
  RNG = CONST * AB * SUM1 / SQRT(PP)
  GRNG = CONST.* CT.* SUM2 / SQRT (P)
  M = 2
  GO TO 19

```



```

57 M = 1
   RNG = 0.0
   GRNG = 0.0
19 DO 29 J = 1,2
   IF ( J .EQ. 2 ) M = 2
   DO 29 I = M, 10
   X1 = ( I - 1 ) * 10 ** ( J - 1 )
   X2 = I * 10 ** ( J - 1 )
C  SUBROUTINE SIMPSON RULE NUMERICAL INTEGRATION
   CALL SIMCON (X1, X2, PREC, 15, RINC, NO1, R, F1)
   CALL SIMCON (X1, X2, PREC, 15, GRINC, NO2, R, F2)
   RNG = RNG + RINC
29 GRNG = GRNG + GRINC
   RNG10 = RNG
   GRNG10 = GRNG
   X1 = (HMAX + HMIN) / 2.0
   DELTA = (HMAX - HMIN) / 2.0
   N = 1
   LIM = 15
   TEST = PREC
   IF (HMIN - XA) 21, 21, 22
21  RNGB = 0.0
   NOIB = 0.0
210 CALL SIMCON ( X0, X1, TEST, LIM, RNGA, NOIA, RA, F1)
   GO TO 23
22  IF (HMIN - XB) 24, 24, 25
24  CALL SIMCON ( X0, XA, TEST, LIM, RNGA, NOIA, RA, F1)
240 CALL SIMCON ( XA, X1, TEST, LIM, RNGB, NOIB, RB, F1 )
   GO TO 23
25  CALL SIMCON ( X0, XA, TEST, LIM, RNGA, NOIA, RA, F1 )
   CALL SIMCON ( XA, XB, TEST, LIM, RNGB, NOIB, RB, F1 )
   DELRNG = ( RNG1 - RNGB - RNGA - RNG10 ) / CONST
   XR = XB + RAD
   RDN3 = THT( A, REF, GRAD, XB, RAD )
   SN3 = SIN ( RDN3 )
   X1 = H3 ( XR, DELRNG, SN3 ) + XB
   H1 = XB / RAD
   PHIC = ARSIN( A * DELRNG / (( 1.0 + H1 ) * ( RAD + X1 )))
   N = 1
   RNG = RNG1
   GO TO 391
23  RNG = RNG10 + RNGA + RNGB
   IF ( N .EQ. MAXN ) GO TO 30
   TESTO = ( RNG - RNG1 ) / RNG1
   TEST1 = ABS (TESTO)
   IF (TEST1 - TEST) 30, 30, 50
30  IF ( HMIN - XA ) 38, 38, 39
38  CALL SIMCON (X0, X1, TEST, LIM, GRNGA, NOIGA, RGA, F2)
   GRNGB = 0.0
   GRNGC = 0.0
   GO TO 37
39  CALL SIMCON ( X0, XA, TEST, LIM, GRNGA, NOIGA, RGA, F2)

```

```

CALL SIMCON ( XA, X1, TEST, LIM, GRNG, NOIGB, RGB, F2 )
GRNGC = 0.0
GO TO 37
391 CALL SIMCON (XO,XA,TEST, LIM, GRNGA, NOIGA, RGA, F2 )
CALL SIMCON (XA, XB, TEST, LIM, GRNGB, NOIGB, RGB, F2 )
GRNGC = PHIC * RAD * CONST
37 GRNG = GRNG10 + GRNGA + GRNGB + GRNGC
THETA = APPA * THT(A, REF, GRAD, X1, RAD )
ALT = X1
TRG = SIN ( GRNG / ( 2.0 * RAD * CONST ))
RFS = SQRT ( ALT * ALT + 4.0 * RAD * (RAD + ALT ) * TRG * TRG )
RNGERR = RNG / CONST - RFS
IF ( ELEV - 45.0 ) 360, 360, 370
360 TRUELV = - APPA * ARSIN ( RFS / ( 2.0 * RAD ) -
1X1 / RFS - ( X1 * X1 ) / (2.0 * RAD * RFS ))
GO TO 380
370 TRUELV = 90.0 - APPA * ( ARSIN((( RAD + X1 ) * ( SIN (
1GRNG / ( RAD * CONST )))) / RFS ))
380 ELEVER = ELEV - TRUELV
HMILES = X1 * CONST
GRG = GRNG
PRINT 31, NN, RNG1, GRG, HMILES, RNGERR, ELEVER
600 FORMAT (1H, 25X, * TROPOSPHERIC PROPAGATION ERRORS IN RADAR MEAS
UREMENTS OF ELEVATION AND RANGE OF TARGET * / 50X, * IONOSPHERE
2ASSUMED NONREFRACTIVE * //
3 60X, * DATA FOR TRIVANDRUM * )
993 FORMAT (1H0, 7X, * ELEV = *, F5.1// 8X, * SL NO *, 5X, * RADAR RA
NGE *, 12X, * GROUND RANGE *, 12X, * HMILES *, 10X, * RANGE ERROR
2*, 5X, * ELEVATION ERROR * / 22X, * (KMS)*, 22X,*(KMS)*,18X,*(Km
3S)*, 14X, *(MRS)*,14X, *(DEGREES)* )
31 FORMAT (1H, 10X, I2, 10X, F6.1, 15X, F11.3, 15X, F8.3, 13X, F6.1
1, 15X, F7.3 )
GO TO 555
50 IF ( N .GT. 1 ) GO TO 60
XN = X1
RNGN = RNG
N = N + 1
DELTA = 0.5 * DELTA
IF ( TEST0 ) 3, 3, 15
3 X1 = X1 + DELTA
GO TO 6
15 X1 = X1 - DELTA
6 IF ( HMIN - XA ) 210, 210, 240
60 XM = X1
X1 = (RNG1-RNGN) * ( X1 - XN ) / (RNG - RNGN ) + XN
XN = XM
RNGN = RNG
N = N + 1
GO TO 6
555 IF ( RNG1 .GT. 95.0) GO TO 333
RNG1 = RNG1 + 10.0
GO TO 101

```

```

333 IF ( RNG1 .GT. 595.0) GO TO 101
    RNG1 = RNG1 + 50.0
101 CONTINUE
    IF (ELEV .GT. 4.9 ) GO TO 225
    ELEV = ELEV + 0.5
    GO TO 5
225 IF (ELEV .GT. 29.0 ) GO TO 230
    ELEV = ELEV + 5.0
    GO TO 5
230 IF ( ELEV .GT. 74.0 ) GO TO 1
    ELEV = ELEV + 15.0
    GO TO 5
499 STOP
    END

```

~~SIBFIC~~ SUB1

```

FUNCTION F1 (X)
C   INTEGRAND FOR SIMCON SUBROUTINE
COMMON /B/ REF, RAD, GRAD, CONST, U, A
    BB = REF * EXP(- GRAD * X)
    CC = X / RAD
    V = 2.0 * BB + BB * BB
    W = 2.0 * CC + CC * CC
    FX = SQRT (U + V + W + V * W )
    F1 = CONST * ( 1.0 + V ) * ( 1.0 + CC ) / FX
    RETURN
END

```

~~SIBFIC~~ SUB2

```

FUNCTION F2(X)
C   INTEGRAND FOR SIMCON SUBROUTINE
COMMON /B/ REF, RAD, GRAD, CONST, U, A
    BB = REF * EXP ( - GRAD * X )
    CC = X / RAD
    V = 2.0 * BB + BB * BB
    W = 2.0 * CC + CC * CC
    FX = SQRT ( U + V + W + V * W )
    F2 = CONST * A / ((1.0 + CC ) * FX )
    RETURN
END

```

~~SIBFIC~~ SIMCON

```

SUBROUTINE SIMCON( X1, XEND, TEST, LIM, AREA, NOI, R, F )
    NOI = 0
    RI = 10.0
    ODD = 0.0
    JNT = 1
    V = 1.0
    EVEN = 0.0
    AREAL = 0.0
19 ENDS = F(X1) + F(XEND)
2 H = ( XEND - X1 ) / V
    ODD = EVEN + ODD
    X = X1 + H / 2.

```

```

      EVEN = 0.0
      DO 3 I = 1, JNT
21  EVEN = EVEN + F(X)
      X = X + H
      3 CONTINUE
31  AREA = (ENDS + 4.0 * EVEN + 2.0 * ODD) * H / 6.0
      NOI = NOI + 1
34  R = ABS ((AREA1 - AREA) / AREA)
      IF (NOI - LIM) 341, 35, 35
341 IF (R - TEST) 35, 35, 4
35  RETURN
      4 AREA1 = AREA
46  JNT = 2 * JNT
      V = 2.0 * V
      GO TO 2
      END

```

```

-
$IBFTC LOGIPL
      SUBROUTINE LOGIPL ( AGT, NSF, SUM )
      ANUM = AGT
      DENOM = 1.0
      SUM = 0.0
1  TERM = ANUM / DENOM
      SUM = SUM + TERM
      TEST = ABS (TERM / SUM)
      IF (TEST - ( 10. ** ( - NSF ))) 2, 2, 3
2  RETURN
3  ANUM = -ANUM * AGT
      DENOM = DENOM + 1.0
      GO TO 1
      END

```

## APPENDIX - B

PROGRAM FOR RANDOM GENERATION OF PSEUDO RANDOM NUMBERS FOR  
SIMULATION OF TROPOSPHERE OVER DELHI.

8IBFTC MAIN

```

C      THIS PROGRAM USES THE SUBROUTINE RADM TO GENERATE 500 PAIRS
C      OF PSEU-DORANDOM NUMBERS IN NORMAL DISTRIBUTION FOR A SET OF
C      VALUES HAVING A MEAN OF 332 N UNITS AND STANDARD DEVIATION
C      OF 25 N UNITS, BASED ON KNOWN NS MONTHLY AVERAGE VALUES FOR
C      DELHI
      INTEGER TAU , ALFA,G, RN1
      REAL MU
      ALFA = 2**18 + 3
C      RN1 = 2**35 - 3 COMPUTED AS BELOW TO AVOID INTEGER OVERFLOW
      RN1 = 2*(2**34-2)+1
      SIGMA = 25.0
      MU = 332.0
      N = 1
      G = 0
      TAU = 3
1    DO 2 I = 1,500
      CALL RADM (SIGMA, MU, TAU, G,N,ALFA, RN1, SN, SN1)
6    THIS PROGRAM IS FOR PRINTING THE NUMBERS
      PRINT 100, SN, SN1
100  FORMAT (2E16.8 )
      2 CONTINUE
      IF (TAU-3) 5,6,5
      5 TAU = TAU + 1
      GO TO 1
      6 STOP
      END

```

8IBFTC RNDM

```

      SUBROUTINE RADM (SIGMA, MU, TAU, G, N, ALFA, RN1, SN, SN1)
      INTEGER, TAU, ALFA, G, RN, RN1
      REAL MU
C      NEXT THREE STATEMENTS PRODUCE INTEGER MOD 2**35 AND THEN CON-
C      VERT THIS TO FLOATING POINT PSEUDORANDOM NUMBER UNIFORMLY
C      DISTRIBUTED ON (0,1).
C      FIRST STATEMENT PRODUCES RESULT MOD 2**35 SINCE THE WATERFOR
C      FORTRAN IV SYSTEM ON THE IBM 7044 IGNORES OVERFLOW IN INTEGER
C      MULTIPLICATION
1    RN = RN1 * ALFA
      RSTN = RN
      RSTN = RSTN * 2.0**(-35)

```

```
C   THE FOLLOWING PROGRAM IS USED TO CONVERT RANDOM NUMBERS
    UNIFORMLY DISTRIBUTED IN THE INTERVAL (0,1) TO NUMBERS
    HAVING NORMAL DISTRIBUTION.
C   IF (G-1) 7,6,7
7  N = N+1
   G = G+1
   RN1 = RN
   RSTN1 = RSTN
   GO TO 1
6  Z = SQRT (-2.0*ALOG(RSTN1))*SIGMA
   SN1 = Z*COS(6.28318*RSTN) + MU
   SN = Z*SIN(6.28318*RSTN) + MU
   G = 0
5  N = N+1
   RN1 = RN
   RETURN
END.
```

# REFERENCES

- [1] Skolnik, Merril I., Radar Handbook, Book, McGraw Hill Book Co., 1970, Chapters 22,24.
- [2] Bean, B.R. and E.J. Dutton, Radio Meteorology, Book, Dover Publications, 1968, Chapters 1,2,3,4,5,8,9.
- [3] Kulshrestha, S.M. and K. Chatterjee, Radio climatology of India, vertical structure of radio refractive index distribution in the lower troposphere, Indian Journal of Met and Geophysics, Part IV, Vol.18, No.3, pp. 335-48, 1967.
- [4] Venkiteshwaran, S.P., etal, Radio refractive index over India and neighbourhood for microwave propagation, RTRC monograph No.1, Feb. 1970.
- [5] Dolubkhanov, M., Propagation of Radio Waves, Book, Mir Publishers, Moscow, 1971, Chapter 3.
- [6] Srivastava, H.N., Some Applications of Radio Characteristics in a tropical standard atmosphere, Proceedings Indian Division of IERE, Vol.V, No.3, pp. 1-4, July-Sep, 1967.
- [7] Venkiteshwaran, S.P., etal, Radio refractivity profile over India, Journal ITE, Vol.15, pp. 395-410, 1969.
- [8] Nathanson, F.E., Radar Design Principles, Book, McGraw-Hill Book Co., 1969, Section 6.7.
- [9] Thayer, G.D., A formula for radio ray refraction in an exponential atmosphere, Journal Res NBS, 65D, No.2, pp. 181-182, Mar-Apr 1961.
- [10] Majumdar, S.C., Some aspects of tropospheric radio refractivity over India, IERE, Vol.38, No.2, pp. 99-108, Aug. 1969.
- [11] Srivastava, H.N. and R.B. Pathak, Regional models of Radio atmospheres over India, Journal of ITE, Vol. 16, No.3, pp. 171-180, 1970.
- [12] Pathak, R.B. and H.N. Srivastava, Models of atmospheric refractive index with reference to coastal stations of India, Indian Journal of Meteorology and Geophysics, Vol.21, No.2, pp. 273-278, 1970.

- [13] Chatterjee, K., Anticipated superrefraction over India based on the climatology of the vertical structure of radio refractivity, Radio Science (USA), Vol.6, No.12, pp. 1033-38, 1971.
- [14] Thayer, G.D., A rapid and accurate ray tracing algorithm for a horizontally stratified atmosphere, Radio Science, Vol. I (New Series), No.2, pp. 249-252, 1967.
- [15] Blake, L.V., Ray height computation for a continuous non-linear atmospheric refractive index profile, Radio Science, Vol.3 (New Series), No.1, pp.85, 1968.
- [16] Rowlandson and Moldt, Derivation of closed functions to compute range and angle errors in an exponential atmosphere, Radio Science, Vol.4, No.10, pp. 927-933, 1969.
- [17] Hopfield, H.S., Two quartic tropospheric refractivity profile for correcting satellite data, Journal of Geophysics Research, 78(18), pp. 4487-4499, 1969.
- [18] Freeman, J., Range error compensation for troposphere with exponentially varying refractivity, Journal of Res., NBS, Sec D, 66(6), pp. 695-679, 1962.
- [19] Marini, J.W., Correction of satellite tracking data for an arbitrary tropospheric profile, Radio Science, Vol.7, No.2, pp. 223-31, 1972.
- [20] Berkowitz, R.S., Modern Radar-Analysis, Evaluation and System Design, Book, John Wiley and Sons, 1965, Part V, Chapter 1.
- [21] Hopfield, H.S., Tropospheric effects on electromagnetically measured range, Radio Science, Vol.6, No.3, pp. 357-367, 1971.
- [22] Skolnik, M.I., Introduction to Radar Systems, Book, McGraw-Hill Book Co., 1962, Chapter 11.
- [23] Vogler, L.E., An approximate height formula for tropospheric ray tracing, IEEE Trans. A and P, pp. 794-796, 1971.
- [24] Levine D., et al, Increase of error in range correction with elapsed time evaluated by ray tracing through radio sonde generated atmospheric models, Radio Science, Vol.18, No.7, pp.633-39, 1973.



- [25] Ralston and Wilf, Mathematical Methods for Digital Computers, Vol.II, Book, 1967, pp. 249-263.
- [26] Srivastava, H.N., Refractivity in the lowest 1 Km over India, Indian Journal of Pure and Applied Physics, Vol.6, No.6, pp. 315-319, 1968.
- [27] Marshall A. Gallop Jr, L.E. Telford, Estimation of tropospheric refractivity bending from atmospheric emission measurement, Radio Science, Vol.8, No.10, pp.819-827, 1973.